Oxygen minimum zones in the Indian Ocean and its responses to changes in the meridional overturning circulation

Eugene Odion Oboh[1,3], Niko Lahajnar[2], Birgit Gaye[2], Avanti Shrikumar[4], Tim Rixen[1]
[1]Leibniz Centre for Tropical Marine Research (ZMT), Bremen, 28359, Germany,
[2]University of Hamburg, Institute for Geology, Hamburg, 20146, Germany,
[3]University of Bremen, Bremen, 28359, Germany,
[4]University of Sydney, Charles Perkins Center, NSW 2006, Australia.

Correspondence to: Eugene Odion Oboh (oboh.eugene@leibniz-zmt.de)

Abstract. The Oxygen Minimum Zones (OMZs) in the northern Indian Ocean (i.e., the Arabian Sea and the Bay of Bengal) are among the most intense OMZs in the world's oceans. While there is no clear evidence of a significant change in the Bay of Bengal OMZ (BoB OMZ)), the Arabian Sea OMZ (AS OMZ) followed the global trend and expanded in the last decades until 2013. Since then, however, this trend has reversed, and the AS OMZ seems to have shrunk. Processes that stabilize the OMZ in the Bay of Bengal and regulate its expansion and contraction in the Arabian Sea are poorly understood. In this study we redefined the source water types (SWTs) and employed an extended optimum multi-parameter (eOMP) analysis to investigate changes in the oxygen supply due to mixing and biological oxygen consumption in these OMZs based on empirical field data from the Global Ocean Data Analysis Project version 2 (GLODAPv2) and a research cruise conducted with a German research vessel Sonne in 2024. Our findings reveal in line with previous studies a reversal in the expansion trend of the AS OMZ but also a shrinkage of the BoB OMZ between 1995 and 2016. In both regions this is due to an increased northward influx of oxygen-rich SWTs from the southern Indian Ocean, combined with a reduced contribution from relatively oxygen-poor local and equatorial SWTs. We also observed that the increased physical oxygen supply was accompanied by enhanced biological oxygen consumption, which partly offsets the effect of the increased oxygen supply on the oxygen concentrations in the OMZs. These changes are likely linked to a reorganization and slowdown of the meridional overturning circulation (MOC) in the Indian Ocean, associated with a weakening of the Asian monsoon and the global thermohaline circulation (THC). The slowdown seems to have increased the residence time of water masses, which is consistent with the enhanced biological oxygen consumption observed, while the weaker zonal circulation appears to have favored the meridional transport of oxygen-rich waters from the southern Indian Ocean northwards. This suggests a coupling between the OMZs in the Indian Ocean and climate-driven changes in the global THC, as also indicated by palaeoceanographic records, although the climate-related drivers differ between past and present.

1 Introduction

The decline of dissolved oxygen in the ocean is one of the greatest threats to the ocean (Breitburg et al., 2018; Oschlies et al., 2018; Schmidtko et al., 2017). It affects biogeochemical cycles, endangers marine ecosystems, and ultimately jeopardizes our food security because many economically relevant marine organisms are animals and need oxygen to breathe (Stramma et al., 2008; Stramma et al., 2010). The declining dissolved oxygen concentration is primarily attributed to global warming and the associated warming of ocean water (Benson and Krause Jr., 1980). This reduces the oxygen solubility and also affects the oxygen minimum zones (OMZs) in the interior of the ocean (Stramma et al., 2008).

OMZs develop mainly below the surface mixed layer in water depths of about 100–600 m as a consequence of the interplay between the physical oxygen supply and the biological oxygen consumption (Sverdrup, 1938). The production of organic matter by phytoplankton, its subsequent export and respiration by bacteria and zooplankton below the photic zone controls the oxygen consumption (Sigman and Hain, 2012; Malone et al., 2015; Rixen et al., 2020). The primary mechanisms supplying oxygen to OMZs are the intrusion of former well-oxygenated surface waters through vertical mixing, variations in the surface mixed layer depth (MLD), as well as isopycnical mixing and the transport of water along density surfaces (Duteil and Oschlies, 2011; Rudnickas et al., 2019). Source water types (SWTs) that ventilate OMZs at lower latitudes are formed at high latitudes in association with the deep and mode water formation (Broecker, 1991; Sarmiento et al., 2004), as well as in regions where evaporation or cooling increases the density of the surface water until it becomes denser than the water below and begins to sink (Reichart et al., 2002). Due to the continuous remineralization of exported organic matter in the water column, oxygen concentrations generally decline as water masses age, with “age” referring to the time elapsed since the water lost contact with the atmosphere (Jeansson et al., 2021; Olsen et al., 2019). Consequently, longer residence times of waters within the OMZ and thus an increase in water ages can enhance oxygen consumption, similar to the effect of an increase in local export of organic carbon (Rixen et al., 2020; Rixen and Ittekkot, 2005; Cavan et al., 2017).

The most intense OMZs occur in the eastern tropical Pacific Ocean, the Arabian Sea, and the Bay of Bengal. The latter two are semi-enclosed basins in the northern Indian Ocean, where dissolved oxygen levels drop below 20 μmol kg^{-1}. (Rixen et al., 2020; Schulz et al., 2025; Acharya and Panigrahi, 2016). This threshold marks the transition from hypoxia to microbial hypoxia, where oxygen concentrations are not only low enough to adversely affect the performance of higher organisms such as fish (Ekau et al., 2010; Vaquer-Sunyer and Duarte, 2008), but also low enough to enable anoxic microbial processes, such as the reduction of nitrate to N_2 (Rixen et al., 2020). Climate projections under all Shared Socioeconomic Pathways predict a decrease in the globally averaged OMZ dissolved oxygen concentration (i.e., water depth between 100–600 m), while projections at the regional level show considerable variations (Kwiatkowski et al., 2020). In particular, the largest decreases in dissolved oxygen concentrations are expected to occur at higher latitudes, while rising oxygen concentrations are projected for equatorial regions. In the Indian Ocean, the increasing equatorial oxygen concentrations have been associated with decreasing oxygen consumption (Kwiatkowski et al., 2020) and the enhanced inflow of oxygen-enriched water masses from the southern

Indian Ocean gyre (Ditkovsky et al., 2023). However, the northern Arabian Sea appears to be an exception with predictions indicating that the OMZ will intensify in the future (Kwiatkowski et al., 2020; Ditkovsky et al., 2023).

Since large parts of the AS OMZ are already in the state of microbial hypoxia, and the BoB OMZ is on the verge of reaching this state (Schulz et al., 2025; Bristow et al., 2017), even minor changes in oxygen concentrations could have significant impacts on the marine nitrogen cycle, the associated marine productivity, and the production of greenhouse gases such as N_2O (Bange et al., 2005). Nevertheless, in line with model results, data collected prior to 2007 reveal an expansion of the AS OMZ (Banse et al., 2014; Goes et al., 2020; Rixen et al., 2014) due to both a reduced ventilation and an increased oxygen consumption. The first was related to the warming and thus a declined inflow of Persian Gulf Water (PGW) into the AS OMZ (Lachkar et al., 2019) and the second was assumed to be a consequence of enhanced biological productivity in surface water in response to an assumed intensification of the Asian summer monsoon (Lachkar et al., 2018). The monsoon-driven upwelling of nutrient-rich deep waters in summer in addition to the deepening of the mixed layer in winter are responsible for the overall high biological productivity in the Arabian Sea and the associated export of organic matter (Brock et al., 1992; Haake et al., 1993; Rixen et al., 2019). However, in contrast to the observed and projected expansion of the AS OMZ, a recent Argo float study showed that the AS OMZ has been shrinking since 2013 due to a decline in surface ocean productivity (Liu et al., 2024). Furthermore, recent observational and modeling studies also noted that in addition to the biological productivity changes in ventilation pathways in combination with large-scale circulation pattern control oxygen variability in the AS OMZ (Oschlies et al., 2017; Vallivattathillam et al., 2023; Lachkar et al., 2019; Narvekar et al., 2025). In particular, shifts in the balance between zonal transport driven by the Indonesian Throughflow (ITF) and Indian Ocean meridional overturning circulation (MOC) may alter the relative contributions of local (i.e., originated in the Arabian Sea and the Bay of Bengal) equatorial, and remote (southern-sourced) SWTs (Ditkovsky et al., 2023). The Bay of Bengal OMZ (BoB OMZ) in turn has remained relatively stable (Johnson et al., 2019; Nayak et al., 2024) as physical forcing mechanisms including salinity stratification, the occurrence of cyclonic, and anticyclonic eddies balance oxygen consumption (Sridevi and Sarma, 2020; Bhaskar et al., 2021).

The OMZs in the northern Indian Ocean are poorly represented in climate models (Rixen et al., 2020; Vallivattathillam et al., 2023) due to uncertainties of almost all processes affecting the OMZs ventilation (Schmidt et al., 2021). The scope of this study therefore, is to investigate changes of the AS and BoB OMZs between 1995 and recent years (i.e., 2016, 2018, 2019, and 2024) using empirical field data. The primary objective is to determine how changes in the composition of SWTs in the OMZs might have triggered the trend reversal of the OMZ in the Arabian Sea after 2013 and contribute to the stability of the BoB OMZ. Therefore, we redefined (i) SWTs, (ii) quantified their contribution to the OMZs using an extended optimum multi-parameter (eOMP) analysis; (iii) quantified the physical oxygen supply, and the (iv) biological oxygen consumption as well as temporal shifts between 1995 and recent years.

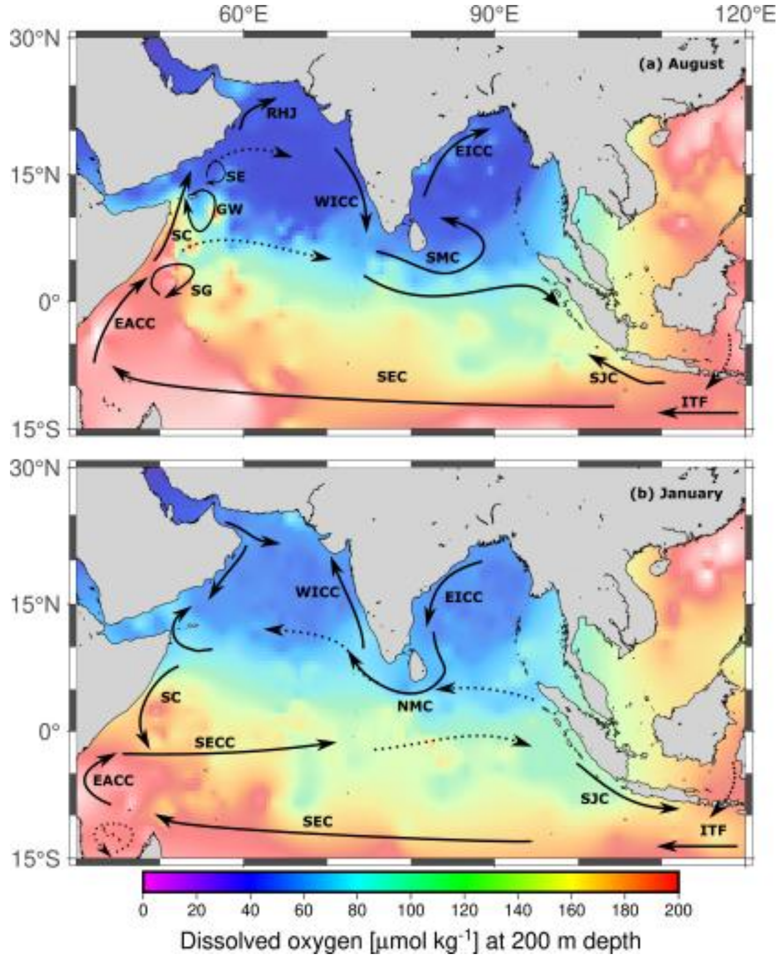

Figure 1: Surface currents in the Indian Ocean during (a) the summer monsoon in August and (b) the winter monsoon in January. Modified from (Schott (Schott et al., 2009). Abbreviations: Somali current (SC), South Equatorial Current (SEC), East African Coastal Current (EACC), Southern Gyre (SG), Socotra Eddy (SE), Great Whirl (GW), Southwest Monsoon Current (SMC), East Indian Coastal Current (EICC), Northeast Monsoon Current (NMC), West Indian Coastal Current (WICC), Indonesian Throughflow (ITF), Ras al Hadd jet (RHJ), South Java Current (SJC).

1.1 Study Area

The Indian Ocean differs from other ocean basins mainly due to its geographical characteristics, which have far-reaching consequences for atmospheric and oceanic circulation. The first unique geographical feature is the Asian landmass. It limits the northern extent of the Indian Ocean in the subtropics at about 30° N and enforces the development of the Asian monsoon. The monsoon is characterized by seasonal changing wind directions (i.e. SW in summer and NE in winter (Gadgil et al., 2007), leading to an overall clockwise surface circulation in summer and a counterclockwise circulation in winter (Fig. 1) (Wyrtki, 1973; Phillips et al., 2021; Schott et al., 2009). The Southwest Monsoon Current in turn carriers Arabian Sea Water into the Bay of Bengal in summer whereas the Northeast Monsoon Currents transports Bay of Bengal water into the Arabian Sea in winter (Fig. 1).

Another unique feature of the Indian Ocean is the Indonesian Archipelago, which allows the inflow of Indonesian

Throughflow Water (ITFW) from the Pacific into the Indian Ocean. It represents the only connection between major ocean basins at low latitudes (Gordon et al., 2010; Gordon et al., 2003) and connects to the outflow of water from the Indian Ocean into the Atlantic Ocean through the Agulhas leakage (Durgadoo et al., 2017; Gordon, 1986). Both, the Agulhas leakage and the ITF act as bottlenecks within the surface water return flow of the global thermohaline circulation (THC) (Durgadoo et al., 2017; Broecker, 1991). The strength of the ITF is sensitive to climate variability, plays a key role in regulating heat and water mass exchange between the two ocean basins, influences the composition of thermocline waters also in both basins as well as the strength of the Agulhas Current (AC) and South Equatorial Current (SEC) in the Indian Ocean (Gordon et al., 2010; Ditkovsky et al., 2023; Lee et al., 2002; Godfrey, 1996). According to numerical model results a blockage of the ITF is weakening the SEC and the AC (Lee et al., 2002).

Contrary to the Atlantic and Pacific Oceans, where major eastern boundary upwelling systems exist off California, NW Africa, Peru and Namibia/South Africa, the only but much weaker upwelling system in the eastern Indian Ocean develops off South Java and Bali (Susanto et al., 2001b, a; Chavez and Messié, 2009; Rixen et al., 2006). However, driven the by strong SW monsoon winds, a coastal upwelling system emerges along the Arabian Peninsula in summer, with an intensity comparable to that of eastern boundary upwelling systems in other ocean basins (Sastry and D'souza, 1972; Brock et al., 1991; Rixen et al., 2019). In summer weaker but also upwelling favorable winds occur along Indian west and east coast in the Arabian Sea and Bay of Bengal, respectively (Abbott and Mahadevan, 2024; Sharma, 1978; Shetye et al., 1990).

The large-scale meridional transport of water masses in the Indian Ocean is governed by the Indian Ocean MOC. It consists of the shallow and deep overturning cells, with the shallow cell encompassing the upper 300–450 m and the deep cell water masses below this depth-range (Schott and Mccreary Jr, 2001; Stramma et al., 2002). The shallow MOC is controlled by monsoon-driven upwelling in the northern Indian Ocean and the formation and subduction of subsurface water masses primarily near the Subantarctic Front in the south (Schott and Mccreary Jr, 2001). The deep MOC is mainly driven by formation of dense water masses in the Southern Ocean, including the Antarctic Bottom Water (AABW) and Antarctic Intermediate Water (AAIW). These water masses spreads northward and contribute to deep and intermediate ventilation in the Indian Ocean (Schott and Mccreary Jr, 2001; Talley, 2013; Haine et al., 1998). Transit times within the shallow MOC are < 7 years (Schmidt et al., 2020), while water masses from the Southern Ocean (i.e., AAIW) take about 9 years to reach the central Indian Ocean and about 30 years to reach the eastern South Indian Ocean (Fine (1993).

New water masses are forming primarily in the southern and northern Indian Ocean. The high salinity Subtropical Surface Water (STSW) forms preferentially north of the Subantarctic Front between 25° S and 35° S and at around 90° E (Wyrtki et al., 1971; Beal et al., 2006) while south of the Subantarctic Front at around 50° S–40° S, low salinity but cool and thus dense water is subducted below the warmer and lighter subtropical water masses (Talley, 1996; Saenko and Weaver, 2001). The AAIW is the deepest of these mode waters. It enters the Indian Ocean through the western boundary around 47° S–39°S and 45° E–80° E (Fine, 1993; You, 1998). The AABW forms around the

Antarctic continental margins (Menezes et al., 2017) and enters the Indian Ocean through the Crozet-Kerguelen gap at depths below 2000m. Since the AABW undergoes significant modification due to mixing in the abyssal Indian Ocean it is referred to as modified Antarctic Bottom Water (mAABW) (Mantyla and Reid, 1995).

In the northern Indian Ocean, the Arabian Sea High Salinity Water (ASHSW) forms preferentially in spring, when the Arabian Sea begins to warm up and the winter MLD flattens out. This water mass typically occurs at depth range between 0–100 m in the Arabian Sea (Kumar and Prasad, 1999). In addition, the Red Sea Water (RSW) and Persian Gulf Water (PGW) from marginal seas, flow through the Gulf of Aden and Gulf of Oman into the Arabian Sea at intermediate depths of approximately 300–1000 m and 250–300 m respectively (Beal et al., 2000; Bower et al., 2000; Tchernia, 1980).

The Indian Ocean is also affected by climate anomalies such as the El Niño-Southern Oscillation (ENSO) (e.g. Bjerknes, 1969, 1966) and Indian Ocean Dipole (IOD) (Saji et al., 1999; Webster et al., 1999). ENSO has far-reaching consequences for the global and coupled circulations in atmosphere and ocean and is often described in terms of sea surface temperature (SST) anomalies in the equatorial Pacific Ocean (**https://psl.noaa.gov/data/timeseries/month**). The IOD, on the other hand, describes anomalies in the difference between SSTs in the eastern and western Indian Ocean. Both the IOD and ENSO influence, amongst many other things, upwelling in the eastern Indian Ocean and the ITF (Rixen et al., 2006; Abram et al., 2003).

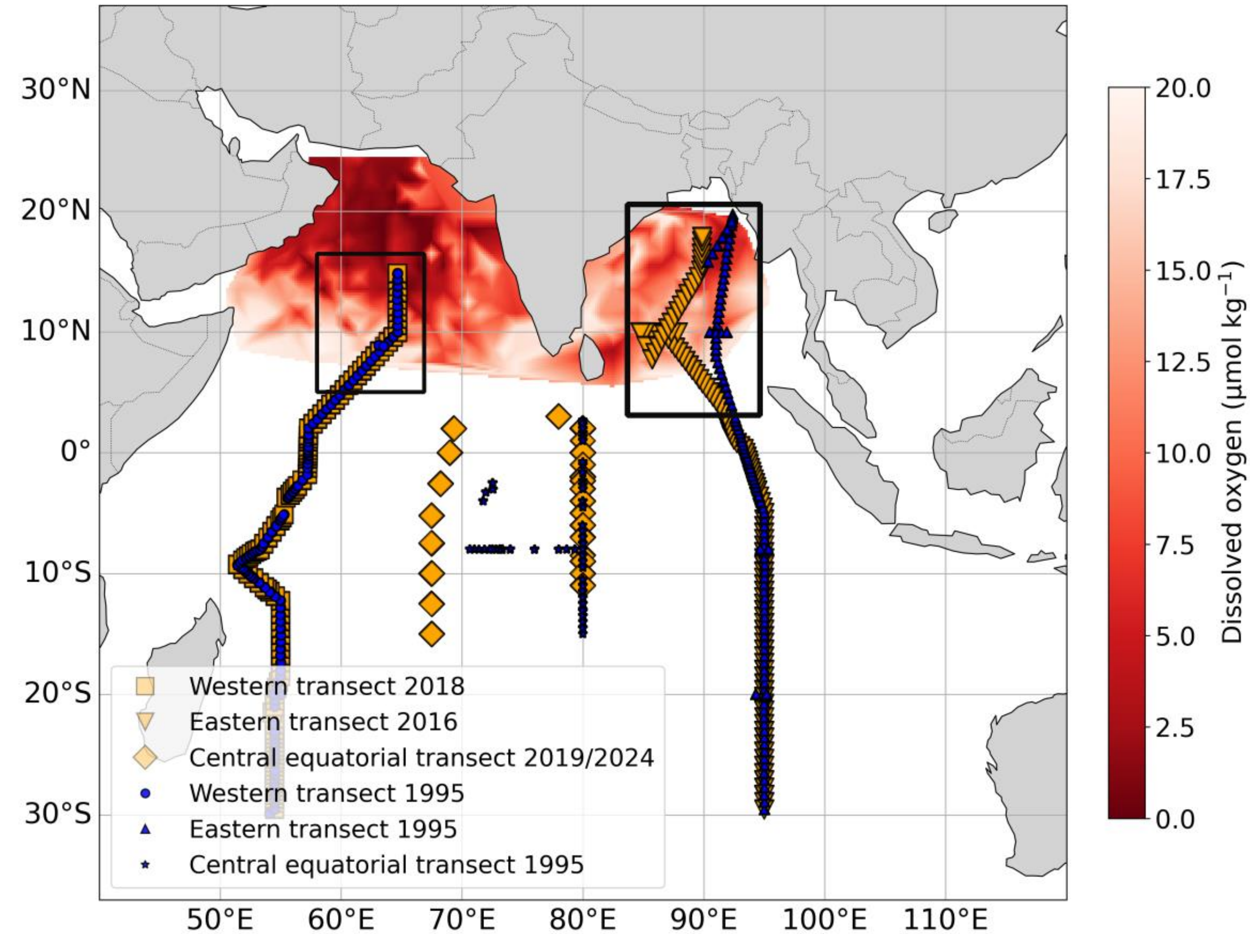

Figure 2: Showing data transect used for extend optimum multi-parameter (eOMP) analysis. western transect (1995 and 2018 GLODAPv2 data), eastern transect (1995 and 2016 GLODAPv2 data), central equatorial transects (1995 GLODAPv2 data) and central equatorial transect (combination of 2024 cruise data and 2019 GLODAPv2 data). Red color map indicates extent of the Arabian Sea and Bay of Bengal oxygen minimum zone cores (O_2 < 20 µmol kg^{-1}) plotted from the WOA data. Solid rectangle highlights portions of the transects used to estimate the OMZs core (O_2 < 20 µmol kg^{-1}) based on the GLODAPv2 data.

2 Methods

2.1 Data collection

The data used in this study were obtained from the GLODAPv2 database (Lauvset et al., 2022; Olsen et al., 2019) and during a cruise with the German research vessel Meteor in the Indian Ocean in 2024, hereafter regarded as cruise data (Gaye et al., 2024). The GLODAPv2 data consists of transects from 1995 and 2018 in the western Indian Ocean, transects from 1995 and 2016 in the eastern Indian Ocean, as well as transects from 1995 and 2019 from the central equatorial Indian Ocean (Fig. 2). We focused on the western and eastern transects because they protrude into the northern Indian Ocean OMZs, therefore, are important in representing the AS and BoB OMZs. The GLODAPv2 data provides oceanographic data from the surface to a depth of 4000 m and includes key parameters such as temperature, salinity, as well as concentrations of dissolved oxygen, nitrate, phosphate, and silicate. We specifically used the merged data product from GLODAPv2, which has undergone extensive quality control, including systematic bias evaluations and corrections for calibration and measurement errors (Olsen et al., 2019). In addition to GLODAPv2, we incorporated cruise data collected near the equator in the central Indian Ocean.

The entire western and eastern transects were analyzed along a depth range between 150 and 1200 m. This filtering enables us to exclude the upper ocean surface waters with a high variability and focus on intermediate depths which aligns with the depth range of OMZs. Furthermore, we defined the core of the OMZs within the transects as regions where the dissolved oxygen concentration falls below 20 µmol kg^{-1}. This corresponds to depths between 150–1000 m for the AS OMZ, and 150–700 m for the BoB OMZ. For the central equatorial region, we compared the 1995 GLODAPv2 data to a combination of the 2019 GLODAPv2 and 2024 cruise data (Fig. 2). The latter were combined to increase the size of the dataset.

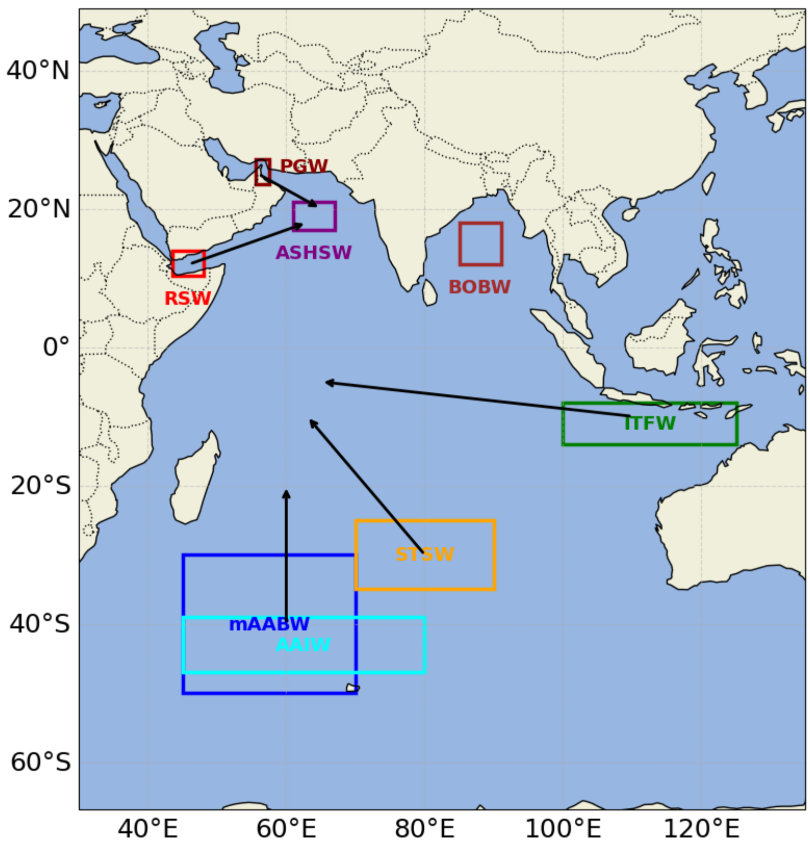

Figure 3. Source water types used in the study, colored rectangular boxes represent region (latitudes and longitudes) where their properties were defined and direction of flow (black arrow). Persian Gulf Water (PGW), Red Sea Water (RSW), Arabian Sea High Salinity Water (ASHSW), Bay of Bengal Water (BOBW), Indonesian Throughflow Water (ITFW), Subtropical Surface Water (STSW), Antarctic Intermediate Water (AAIW), modified Antarctic Bottom Water (mAABW)

2.1.1 Primary productivity, sea surface temperature data as well as ENSO and IOD indicators

Ocean primary productivity data from (Kulk et al., 2020) was used to analyze productivity in the Arabian Sea. The data was accessed on March 26, 2025 and consists of monthly global marine phytoplankton primary production data at a 9 km resolution between 1998–2020. This data was filtered for the Arabian Sea (5° N–25° N, 50° E–75° E) and equatorial Indian Ocean (8° S–8° N, 55° E–85° E) and the annual mean was plotted to observe the trend (Supplement Fig. S1). Likewise, sea surface temperature (SST) data from NOAA was accessed on July 20, 2025. It consists of weekly mean SST data from 1981 to 2025 at a resolution of 0.25°. We filtered this data for the Indian Ocean region (30° N–30° S, 30° E–120° E) and plotted the yearly mean SST and 5-years running mean SST to observe the trend across the Indian Ocean (Supplement Fig. S2). Furthermore, the Oceanic Niño Index (ONI) and IOD or Dipole Mode Index have been downloaded from: **https://psl.noaa.gov/data/timeseries/month/.** The ONI represents SST anomalies in the tropical Pacific Ocean (5° N–5° S, 120° W–170° W) and the IOD shows anomalous in the SST gradient between the western (50° E–70° E and 10° S–10° N) and eastern Indian Ocean (90° E–110° E and 10° S–0° N).

2.2 Source water types selection and definition

It is important to define SWTs properties when performing eOMP analysis, as the latter relies on precise SWTs definition in order to quantify mixing proportions and biogeochemical processes, as it involves modelling a water sample as a linear combination of different SWTs (Shrikumar et al., 2022; Tomczak and Large, 1989). A SWT is an identifiable body of water with distinct physical and chemical properties (e.g., temperature, salinity, as well as concentrations of oxygen and nutrients) that originates from a specific formation region and/or has a specific mixing history (Tomczak, 1999). These properties act as conservative or non-conservative tracers, which makes it possible to track the SWT movement (Tomczak, 1999).

The definition of SWTs in the Indian Ocean is challenging. Many studies are based on secondary SWT rather than primary SWTs (Acharya and Panigrahi, 2016; Ditkovsky et al., 2023; Narvekar et al., 2025). Following the definition of water mass ages (Jeansson et al., 2021; Olsen et al., 2019), a primary SWT is formed when water is introduced into the ocean interior and becomes decoupled from atmospheric influence. Secondary SWTs are mixtures such as Indian Central Water (ICW) and Subantarctic Mode Water (SAMW). We have focused on primary SWTs since they are essentially responsible for the ventilation of the OMZs and carry the influence of global warming on their properties into the depths of the ocean. Nevertheless, secondary SWTs such as ICW and SAMW have not been excluded in our selection. Their influence is fully represented through their parent source components (i.e., the STSW and AAIW) (Tomczak and Large, 1989; You, 1998; Schott and Mccreary Jr, 2001; Sokolov and Rintoul, 2002; Vianello et al., 2017). However, properties of primary SWTs must be defined at the sites of origin, including a geographic area, a characteristic depth range, and, in some cases, a specific time of year. These variables are not precisely constrained; they may also shift in response to climate change and are therefore typically estimated to the best of our current knowledge. Based on a literature review we summarized the specific latitude, longitude and depth ranges for all SWT of relevance for the ventilation of the OMZ in the northern Indian Ocean in Table 3 and marked the region of origin/definition in Figure 3.

Eight SWTs were selected for our initial analysis, including; PGW, STSW, mAABW, ITFW, AAIW, ASHSW, RSW, and Bay of Bengal Water (BOBW) since they are known to influence the OMZ in the Indian Ocean (Chinni et al., 2019; Sabu et al., 2015; Singh et al., 2012; Yu et al., 2018; Song et al., 2004; Beal et al., 2000; Bower et al., 2000; Prasad et al., 2001). The mAABW is an exceptions as it enters the Indian Ocean not as a primary SWT but as a deep water mass which, as motioned before, undergoes significant modification due to mixing in the abyssal Indian Ocean (Mantyla and Reid, 1995). However, due to its relevance for the ventilation of the northern Indian Ocean and in particular the deep MOC (Song et al., 2004; Johnson, 2008) it cannot be ignored in the eOMP analysis.

2.2.1 World Ocean Atlas data

Since the GLODAPv2 data lacks coverage in the key source regions where the relevant SWTs form or enter into the Indian Ocean, SWT properties were derived from World Ocean Atlas (WOA) annual statistical mean data. This data consists of ¼° grid annual average temperature and salinity data from time periods 1995–2004 and 2015–2022, 1° annual average oxygen concentration data from 1971–2000, and 1° grid annual average nutrient concentration data from 1965–2022. We acknowledge that data interpolation can add some uncertainty. However, analysis of WOA "numbers of observation" data shows high density of observations in regions where the SWTs were defined.

In order to take global change impacts into account when defining SWTs property we used the WOA 1995–2004 data as well as WOA 2015–2022 data to define the temperatures and salinity of the SWTs. Since there are no decadal averages in the WOA data for oxygen and nutrients, we defined the nutrient concentration of SWTs using the WOA "All time periods" data (1965-2022) for both 1995 and recent years eOMP analysis. This means that we assume that concentration of nutrients in the near-surface layer of the ocean, where SWTs form, has not changed. Although this assumption cannot be proven, it is supported by the lack of evidence of a change in the CO_2 uptake by the biological carbon pump, which is closely linked to the availability of nutrients. Furthermore, since primary SWTs are not formed by the mixing of different water types (such as ICW), changes in nutrient concentrations resulting from varying mixing ratios should also be negligible. However, unlike nutrient concentration, changes in oxygen concentration can be assumed, as the solubility of oxygen depends on temperature and salinity. We therefore defined the SWTs oxygen concentration using the 1971–2000 WOA oxygen data for the 1995 eOMP analysis, while for eOMP analysis of recent years, we calculated the SWTs oxygen concentration in a manner that accounts for potential climate-driven changes in oxygen, as described below.

2.2.2 Changes in source water types oxygen calculation

Oxygen saturation concentrations for 1995 and recent years were calculated from the corresponding temperature and salinity of each SWT using the formulation of Benson and Krause Jr (1984). The resulting values were converted from µmol L^{-1} to µmol kg^{-1} using seawater density derived from the UNESCO equation of state at atmospheric pressure. Differences in oxygen saturation concentration between 1995 and recent years were interpreted as changes in oxygen.

As most of these changes were negative (with the exception of AAIW), consistent with reported global ocean deoxygenation driven by warming (Schmidtko et al., 2017), we subtracted the calculated oxygen changes from the SWT oxygen values derived from the WOA 1971–2000 data to estimate SWT oxygen values for recent years. Accordingly, WOA (1971–2000) SWT oxygen values were used for the eOMP analysis of 1995, while the adjusted SWT oxygen values (i.e., 1995 values minus the calculated oxygen change) were used for the eOMP analysis of recent years (see Table 2).

As noted above, not only long-term global warming but also climate anomalies, such as ENSO and the IOD, can influence surface water properties via e.g., their effect of energy fluxes across the ocean atmosphere interface. However, defining properties of primary SWTs based on decadal averages, intended to represent the signal of global warming, may therefore be problematic when comparing individual years that are affected by strong climate anomalies. In this study, we compare 1995 with 2016 (eastern Indian Ocean transect), 2018 (western Indian Ocean transect), and 2019 (equatorial Indian Ocean transect). Although early 2016 was marked by a strong El Niño event, the annual mean ONI, similar to 2018 and 2019, indicates only weak to moderate El Niño conditions overall. In contrast, 1995 was characterized by weak La Niña conditions. The IOD index likewise suggests generally moderate conditions in 1995, 2016, and 2018, whereas 2019 experienced a pronounced positive IOD phase (Supplement Fig. S3). We therefore assume that climate anomalies did not exert a dominant influence on the interpretation of data from the western and eastern Indian Ocean, whereas their impact should be considered when interpreting the eOMP results for the equatorial Indian Ocean.

2.3 Optimum multi-parameter (OMP) analysis

The OMP analysis is a mathematical technique developed by Tomczak and Large (1989) to study water mass mixing in a given region. In this approach, a water sample is considered to be a mixture of multiple SWTs. The objective of the analysis is to determine the fraction of each SWT in the water sample. This is achieved by using a non-negative least square method to estimate the contribution of each SWT for a given measurement point of the sample. For this study we performed an eOMP analysis which unlike the classic OMP analysis, considers biogeochemistry. The eOMP analysis was performed using a Python-based model called PYOMPA (Shrikumar et al., 2022). PYOMPA is based on the original OMP analysis by Tomczak and Large (1989). The mathematical formula used to solve the objective function is presented in Eq. (1):

$$\left(\sum_i e_p^i x_j^i\right) + r_B^A \Delta_j^B = s_p^j + \epsilon_p^j \quad (1)$$

Here, s_p^j denote the value of the property p in measured water sample j,

x_j^i stands for the estimated fraction of SWT i in water sample j,

e_p^i stands for the value of property p *in the* SWT,

ϵ_p^j denotes the residual in explaining property p for sample j,

$r_B^A \Delta_j^B$ represents the biogeochemical terms, where r_B^A denotes the exchange ratio of two properties *A* (oxygen) and *B* (phosphate and nitrate), while Δ_j^B denotes the amount of property *B* that is re-mineralized due to the consumption of property *A* in sample *j*.

The residual equation is presented in Eq. (2), where μ_p represent the property mean.

$$\epsilon_p^j = \frac{W_p^{user}}{\sigma_p}\left(\left(\sum_i \left(e_p^i - \mu_p\right) x_j^i\right) + r_B^A \Delta_j^B - \left(s_p^j - \mu_p\right)\right) \quad (2.)$$

To regulate the effect of any properties on the equation, weights were assigned to each property. The bigger the weight, the higher its influence on the eOMP solution. Weights were adopted from Acharya and Panigrahi (2016) and reflect the relative analytical uncertainty and quasi-conservative behavior of each tracer in the Indian Ocean OMZs, with higher weights assigned to temperature and salinity and lower weights to non-conservative biogeochemical properties (see Table 2).

2.3.1 Determined eOMP solution

In order to achieve a determined eOMP solution, we reduced the number of SWTs to six by means of an exclusion process. First, we performed a preliminary underdetermined eOMP analysis using the entire eight SWTs as mentioned above. Thereafter, we separated the SWTs into major SWTs (PGW, STSW, mAABW, ITFW) and minor SWTs (AAIW, ASHSW, RSW and BoBW) based on their contributions in the Arabian Sea OMZ. Then, we performed four sets of overdetermined eOMP analysis using five SWTs and seven constraints (temperature, salinity, oxygen, phosphate, nitrate, silicate and mass). The five SWTs included four major SWTs that were kept constant plus one minor SWTs at a time. Using this method, we identify PGW, RSW, STSW, mAABW and ITFW as the major contributors to the OMZ with the least residuals, and the combination of PGW, RSW, STSW, mAABW, ITFW and AAIW as the major contributors in the entire western Indian Ocean transect with the least residuals (Supplement Fig. S4, S5). Since these six SWTs resulted in even smaller residuals in the eastern Indian Ocean transect, we adopted them in the final eOMP analysis for all transects.

2.3.2 Sensitivity of eOMP solution to variability in source water types property

To evaluate the sensitivity of the eOMP solution to variability in SWT oxygen concentrations, we conducted an oxygen sensitivity test, where we used a higher oxygen scenario (i.e., we added the calculated oxygen change described earlier to the 1995 oxygen values), a constant oxygen scenario (i.e., we used the 1995 oxygen values for eOMP analysis of recent years), and a lower oxygen scenario (where the oxygen change was subtracted). The resulting SWT fractions and changes between 1995 and recent years were not significantly different (Supplement Fig. S6). Therefore, variability in SWT oxygen concentration doesn't alter the conclusion of this study.

We also performed SWTs property variability test to understand how the SWTs fractions derived from eOMP analysis is affected by variability in their properties. To achieve this, we defined all the selected six SWTs using literature values according to Table 1 (see Table S1 in Supplement for the SWTs properties used in the sensitivity analysis). We performed the sensitivity analysis using the 2018 western transect. The result does not differ significantly (Supplement Fig. S7), as the major SWTs contribution remained similar to the output when SWTs properties were defined using WOA data according to Table 2.

2.3.3 Sensitivity of eOMP solution to remineralization ratios and parameter weights

We performed a sensitivity analysis to assess the sensitivity of the eOMP solution to O_2:PO_4:NO_3 remineralization ratios as well as to the parameter weights. For the remineralization ratios, we performed sensitivity analysis based on three O_2:PO_4:NO_3 ratio scenarios, -138:1:16 (the standard Red field ratios), -155:1:15 (Hupe and Karstensen, 2000), and -170:1:16 (Anderson and Sarmiento, 1994). For each scenario, we computed the model's root mean square (RMS) error from its total weighted sum of squared residuals and also computed the mean fraction of SWTs. The results revealed that the scenario with the lowest oxygen ratio (i.e., O_2: −138) led to the highest RMS errors and a more varied distribution of SWTs compared to the other two scenarios, while ratios with O_2: -170 and O_2: -155 both had similar RMS and SWTs distribution (Supplement Fig. S8), we selected −155:15:1 because it recorded the least RMS and align more closely with standard Redfield stoichiometry. Additionally, we conducted sensitivity analysis to evaluate how variations in individual parameter weights from Acharya and Panigrahi (2016) influence model solution. Each weight (e.g., for temperature, salinity, oxygen, phosphate, nitrate and silicate) was independently varied by ± 3 units from its baseline value while all other weights remained fixed. All runs used constant remineralization ratios (O_2:PO_4:NO_3 = −155:1:15). For each scenario, we computed the model's RMS error and mean SWT fractions. The results show that the model was more sensitive to changes in nutrient and relatively stable to changes in temperature and salinity (Supplement Fig. S9). Finally, we adopted the parameter weights from Acharya and Panigrahi (2016) because, despite higher sensitivity to variations in nutrient weights, the overall SWTs contributions remained relatively stable, indicating a robust solution.

Remineralization was tracked as a conversion of oxygen to phosphate and nitrate according to the ratio -155:1:15, adopted from Hupe and Karstensen (2000). The low parameter residue in objective and low mass residual in the OMZs (< 0.003) recorded by the majority (>98.7%) of the water samples show that the water samples were well represented by the SWTs included in the eOMP analysis (Poole and Tomczak, 1999; Shrikumar et al., 2022).

2.4 Physical oxygen supply and biological oxygen consumption analysis

Physical oxygen supply analysis determines the amount of oxygen (O_2) in the sample (*j)* supplied via mixing by a specific SWT ($s^j_{iO_2}$). Therefore, the fraction of the SWT (x^i_j) in the measured sample, *j* was multiplied by the defined oxygen concentration of the SWT ($e^i_{O_2}$) according to Eq. (3).

$$s^j_{iO_2} = x^i_j \text{ x } e^i_{O_2} \quad (3)$$

Oxygen consumption in this study represents the net biological oxygen utilization and it is closely related to Apparent Oxygen Utilization (AOU). Biological oxygen consumption in a given sample (*j)* due to remineralization ($s^{j}_{-O_2}$), was calculated using the measured oxygen in the sample ($s^{j}_{O_2}$), and the overall oxygen due to mixing of all SWTs $\left(\sum s^{j}_{nO_2}\right)$ according to Eq. (4):

$$s^{j}_{-O_2} = s^{j}_{O_2} - \left(\sum s^{j}_{nO_2}\right) \quad (4)$$

The oxygen consumption term is exactly equal to the remineralization term calculated within the eOMP solution when the oxygen residual is added. We calculated the physical oxygen supply and biological oxygen consumption for the OMZ core which corresponds to depth range of 150–1000 m for AS OMZ and 150–700 m for BoB OMZ. As well as for the entire western and eastern transects (150–1200 m) and equatorial transects (15° S–3° N, 150–1200 m).

Table 1. Literature values of source water types (SWTs) property

SWTs	References	Potential Temp. (°C)	Salinity	PDA (kg m^{-1})	Oxygen (µmol kg^{-1})	Phosphate (µmol kg^{-1})	Nitrate (µmol kg^{-1})
PGW	Acharya and Panigrahi (2016)	18.11	36.5	-	43.75	2.12	21.05
	Kumar and Prasad (1999)	19-13	37.9-35.1	26.2-26.8	-	-	-
AS PGW	Coatanoan et al 1999	15	35.8	26.59	9	2.4	20
AS RSW		10	35.3	27.18	22.33	2.6	30
RSW	Acharya and Panigrahi (2016)	12.55	36.2	-	28	2.38	30.46
	Kumar and Prasad (1999)	11-9	35.6-35.1	27.0-27.4	-	-	-
PGW/RSW	Hupe and Karstensen (2000)	18.7	37.69	~ 27.1	50	1.56	19.7
	You and Tomczak (1993)	25.9	38.08	25.7	161.9	0.372	-
	Rixen and Ittekkot (2005)	27.41	36.33	-	146.5	0.99	8.67
RSIW	You (1998)	11.96	35.63	27.13	23.96	2.55	-
mAABW	Haine et al. (1998)	0.8	34.72	28.14	245	-	-
dIDW	Acharya and Panigrahi (2016)	0.92	34.72		221.47	2.12	30.53
LIDW	Hupe and Karstensen (2000)	0.38	34.7		216	2.2	32.1
ICW	Coatanoan et al. (1999)	10.2	34.8	26.76	250	0.8	8
	Rixen and Ittekkot (2005)	12.45	35.11	< 25	126.3	1.46	21.21
ICW upper	Acharya and Panigrahi (2016)	18	35.47		253.41	0.11	0.01
ICW lower		9	34.54		274.37	1.07	14.39
AAIW	You (1998)	7.04	34.48	27.12	233.97	1.59	-
	Vianello et al. (2017)	6	34.6	-	-	-	-
	De Brauwere et al. (2007)	3.8-4.0	34.35-34.25	-	-	-	-
	Harms et al. (2019)						28.57
ASHSW	Kumar and Prasad (1999)	28-24	36.7-35.3	22.8-24.5	-	-	-
	Vianello et al. (2017)	28-24	35.45-35.3	-	196	-	-
ITFW	Vianello et al. (2017)	17-20	35.2	-	108.93	-	-
IIW	You (1998)	8.16	34.69	27.13	76.25	2.28	-

ITFW	Ayers et al. (2014)						13.31
STSW	De Brauwere et al. (2007)	13.28-	35.34-34.71	-	-	-	-
	Sokolov and Rintoul (2002)	12.94	35.30-35	-	-	-	-
	Harms et al. (2019)	11-16.25			200	2.29	2.85
BOBW	Parvathi et al. (2014)	10-5	35.1-35.0	26-27	-	-	-
BOBW	Sengupta et al. (2013)	24.23-29.66	24.97-34.96	-	-	-	-

IIW- Indonesian Intermediate water, RSIW – Red Sea Intermediate Water, LIDW – Lower Indian Deep Water dIDW – deep Indian Deep Water, AS PGW – Arabian Sea Persian Gulf water, AS RSW – Arabian Sea Red Sea water

Table 2. Properties of source water types (SWTs) included in this study and their associated weights in the eOMP solution.

SWTs	Potential Temp. (°C)	Absolute Salinity	PDA (kg m^{-1})	Oxygen (µmol kg^{-1})	Phosphate (µmol kg^{-1})	Nitrate (µmol kg^{-1})	Silicate (µmol kg^{-1})
PGW	21.07[a] 21.39[b]	36.56[a] 36.73[b]	25.67[a] 25.71[b]	36.85[c] 35.45[d]	1.87	18.94	14.64
RSW	14.50[a] 14.90[b]	36.37[a] 36.35[b]	27.14[a] 27.04[b]	25.58[c] 23.78[d]	2.09	27.47	31.29
mAABW	1.18[a] 1.2[b]	34.9[a] 34.9[b]	27.95[a] 27.95[b]	210.29[c] 210.09[d]	2.20	31.43	117.06
AAIW	6.18[a] 6.02[b]	34.52[a] 34.52[b]	27.15[a] 27.17[b]	211.41[c] 210.31[d]	1.87	29.67	34.19
ASHSW	24.23[a] 24.33[b]	36.45[a] 36.39[b]	24.67[a] 24.60[b]	122.82[c] 122.62[d]	1.00	11.95	6.72
ITFW	18.10[a] 18.19[b]	34.55[a] 34.59[b]	24.91[a] 24.92[b]	131.92[c] 131.52[d]	1.04	14.09	21.34
STSW	14.08[a] 14.78[b]	35.35[a] 35.41[b]	26.44[a] 26.34[b]	236.40[c] 233.00[d]	0.55	5.72	3.45
BOBW	16.39[a] 16.69[b]	34.92[a] 34.90[b]	25.60[a] 25.52[b]	20.85[c] 19.55[d]	2.11	25.56	31.15
Weights	36	36		14	5	5	1

PDA= Potential density anomaly with respect to a reference pressure of 0 dbar,
a = SWT properties defined using 1995–2004 WOA data
b = SWT properties defined using 2015–2022 WOA data
c = SWT oxygen properties defined using 1971–2000 WOA data
d = SWT oxygen properties calculated from oxygen change according to Benson and Krause Jr (1984)

Table 3. The specific latitude, longitude and depth ranges used for source water types (SWTs) definition.

SWTs	Latitude	Longitude	Depth range
PGW	23.6° N–27.1° N	55.5° E–57.5° E	100–300m
RSW	10.3° N–14° N	43.5° E–48° E	300–800 m
mAABW	50° S–30° S	45° E–70° E	3000–5500 m
AAIW	47° S–39° S	45° E–80° E	500–1000 m
ASHSW	17° N–21° N	61° E–67° E	50–100 m
ITFW	14° S–8° S	100° E–125° E	80–300 m
STSW	35° S–25° S	70° E–90° E	100–300 m
BOBW	12° N–18° N	85° E–91° E	100–250 m

3 Results

3.1 Source water types composition and temporal changes in the Indian Ocean

The primary objective of this study is to investigate changes of the Arabian Sea and Bay of Bengal OMZs between 1995 and recent years (2016–2024). First, we will consider changes in the composition of SWTs, focusing on how contributions from remote sources (i.e., SWTs with southern Indian Ocean pathway), equatorial sources (i.e., ITFW), and local sources (i.e., SWTs formed in the northern Indian Ocean) have changed between 1995 and recent years (2016–2024).

3.1.1 Spatial distribution and regional differences in 1995

The spatial distribution of SWTs composition across the Indian Ocean in 1995 reveals distinct regional patterns that reflect varying influences of remote and local SWTs. In the western Indian Ocean transect (15° N–30° S, 150–1200 m), the dominant SWTs were STSW (39 %), mAABW (30 %), and AAIW (10 %). Contributions from ITFW (8 %) and PGW (9 %) were also notable, whereas contribution from RSW (4 %) was relatively minimal (Fig. 4c). In the central equatorial Indian Ocean (3° N–15° S, 150–1200 m), analysis revealed a slightly similar structure, with dominant influence from mAABW (40 %), STSW (31 %), ITFW (15 %), and AAIW (8 %). PGW (3 %) and RSW (3 %) contributions were minimal (Fig. 4g). In the eastern Indian Ocean transect (15° N–30° S, 150–1200 m), mAABW (36 %) was the most significant contributor followed by STSW (30 %), ITFW (13 %), and AAIW (11 %). PGW (7 %) and RSW (3 %) were present in relatively smaller proportions, similar to the western transect (Fig 4f).

3.1.2 Distinct characteristics of the Arabian Sea and Bay of Bengal OMZs in 1995

The Arabian Sea and Bay of Bengal OMZ cores ($O_2 < 20$ µmol kg^{-1}) are located in the northern part of both the western and eastern transects. These OMZs also exhibit notable differences in their SWTs distribution in 1995. Unlike in the western transects, the AS OMZ was strongly influenced by PGW (28 %), mAABW (27 %), STSW (24 %), and RSW (14 %), with lesser contributions from ITFW (6 %) and AAIW (1 %) (Fig. 4a). In contrast, the BoB OMZ was dominated by mAABW (34 %), STSW (27 %), ITFW (21 %), and PGW (14 %). Contributions from RSW (1 %), AAIW (3 %), were all relatively minor (Fig. 4d).

3.1.3 Temporal shifts in source waters contribution.

Over the comparison period, the data reveal a consistent and region-wide shift from local and equatorial SWTs towards remote southern-origin waters. Across the western Indian Ocean transect, contributions from STSW and AAIW increased from 39 % to 42 % and 10 % to 13 % respectively, between 1995 and 2018. In contrast, the proportions of PGW, RSW, ITFW, and mAABW all declined (Fig. 4c).

Within the core of AS OMZ, the contribution of PGW declined from 28 % to 22 %, whereas STSW increased from 24 % to 26 % between 1995 and 2018. Over the same period, mAABW (27 % to 26 %) and ITFW (6 % to 4 %) showed modest decreases, while RSW increased from 14 % to 17 %. AAIW contributed only marginally but showed a small increase (Fig. 4a). Although not included in the final analysis, determined eOMP analysis incorporating BoBW and ASHSW also indicate declines in these SWTs across the western Indian Ocean and AS OMZ between 1995 and 2018 (Supplement Fig. S4).

In the eastern Indian Ocean transect, between 1995–2016, a similar trend was observed. The contribution of STSW increased from 30 % to 35 %, additionally, mABBW and AAIW also showed slight increases. However, contributions from PGW (7 % to 5 %), RSW (3 % to 1 %), and ITFW (13 % to 11 %) all declined (Fig. 4f). Furthermore, within the same time period in the core of BoB OMZ, STSW and AAIW increased from 27 % to 35 % and 3 % to 6 % respectively, while PGW (14 % to 9 %), ITFW (21 % to 20 %), and mAABW (34 % to 28 %) all declined. Contribution from RSW (1 % to 2 %) was very minimal but showed an increase just like in the AS OMZ (Fig. 4d).

Table 4. Percentage change in source water types (SWTs) composition in the Arabian Sea OMZ (AS OMZ) and Bay of Bengal OMZ (BoB OMZ).

SWTs	Source Region	Category	AS OMZ Δ% (1995–2018)	BoB OMZ Δ% (1995–2016)	Interpretation
STSW	25–35° S, Subtropical South Indian Ocean	Remote	↑ 8 %	↑ 30 %	Enhanced shallow cell of the Indian Ocean MOC
AAIW	Subantarctic Front	Remote	↑ 5 %	↑ 100 %	Enhanced shallow–intermediate cell of the Indian Ocean MOC
RSW	Red Sea	Local	↑ 21 %	↑ 100 %	Enhanced shallow cell of the Indian Ocean MOC.
PGW	Persian Gulf	Local	↓ 21 %	↓ 35 %	Shoaling/stratification of regional seas
ITFW	Indonesian Archipelago	Equatorial	↓ 33 %	↓ 5 %	Decline of Indonesian Throughflow (ITF)
mAABW	Antarctic/Southern Ocean	Remote	↓ 4 %	↓ 18 %	Weakening of the deep Indian MOC

Temporal changes in the equatorial Indian Ocean (3° N–15° S) also follow these basin-wide shifts. In the western equatorial transect, between 1995–2018, increases in STSW (40 % to 43 %) and AAIW (9 % to 12 %) were observed, while mAABW (35 % to 33 %), PGW (4 % to 3 %), RSW (2 % to 1 %), and ITFW (10 % to 8 %) declined (Fig. 4b). Between 1995 and 2019/2024, the central equatorial region showed a similar pattern, with STSW (31 % to 41 %) increasing, while all other SWTs decreased (Fig. 4g). In the eastern equatorial region between 1995 and 2016, all local and equatorial SWTs declined. However, STSW (30 % to 35 %) and mAABW (37 % to 39 %) increased (Fig. 4e).

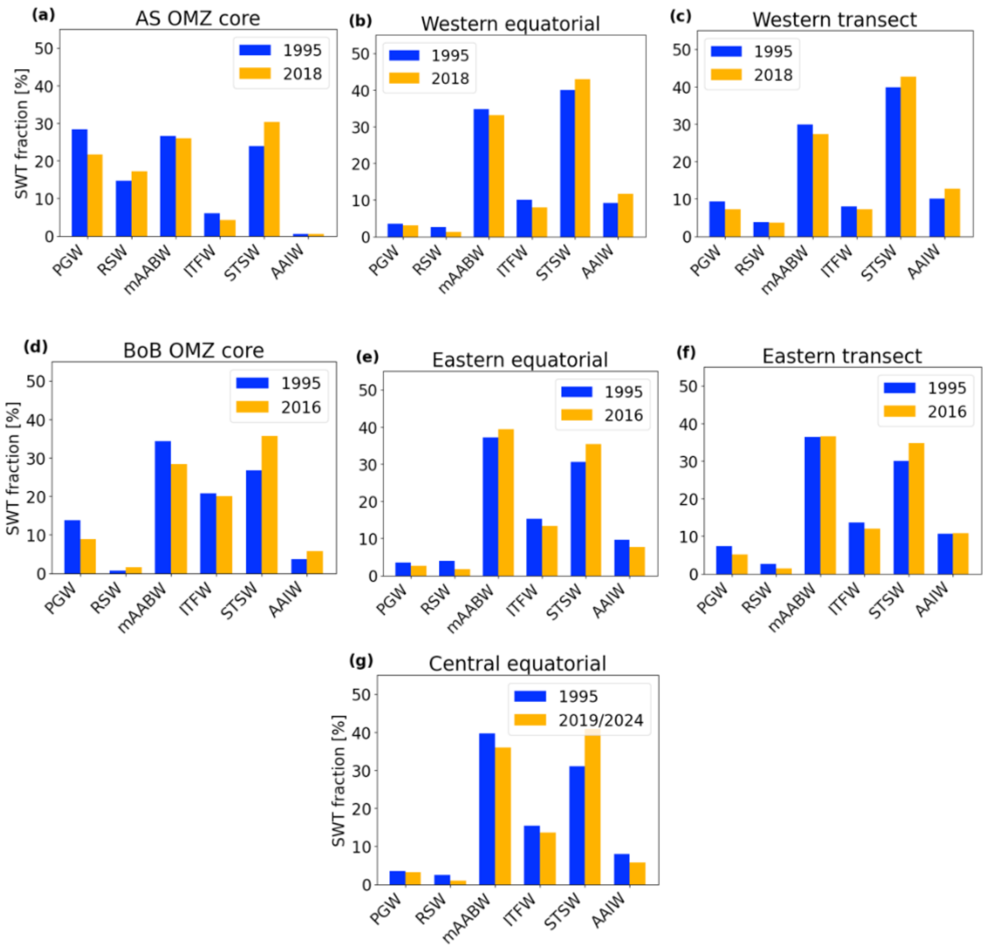

Figure 4: Source water types (SWTs) fraction in the Indian Ocean (a) Arabian Sea OMZ (O_2 < 20 µmol kg^{-1}, depth 150–1000 m), (b) western equatorial region (15° S–3° N, depth 150–1200 m), (c) entire western transect (150–1200 m), (d) Bay of Bengal OMZ (O_2 < 20 µmol kg-1, depth 150–700 m), (e) eastern equatorial region (15° S–3° N, depth 150–1200 m) (f) entire eastern transect (150–1200 m), (g) central equatorial region (15° S–3° N, depth 150–1200 m).

A vertical section of the ITFW contribution clearly shows a temporal decline especially between 10° S–20° S across all transects (Fig. 5). Overall, there is a noticeable decline of the ITFW across the transects from east to west and towards the northern Indian Ocean (Fig. 5). The effect of the ITFW decline is noticeable in the distribution of the STSW in the recent years across all transect. The penetration of STSW is evidently increased at lower depths between 500–800 m and around 10° S–20° S in 2016/2018 compared to 1995 (Fig. 6). Overall, there is an increase in STSW fraction from around 15° S toward the northern Indian Ocean across all transects (Fig. 6).

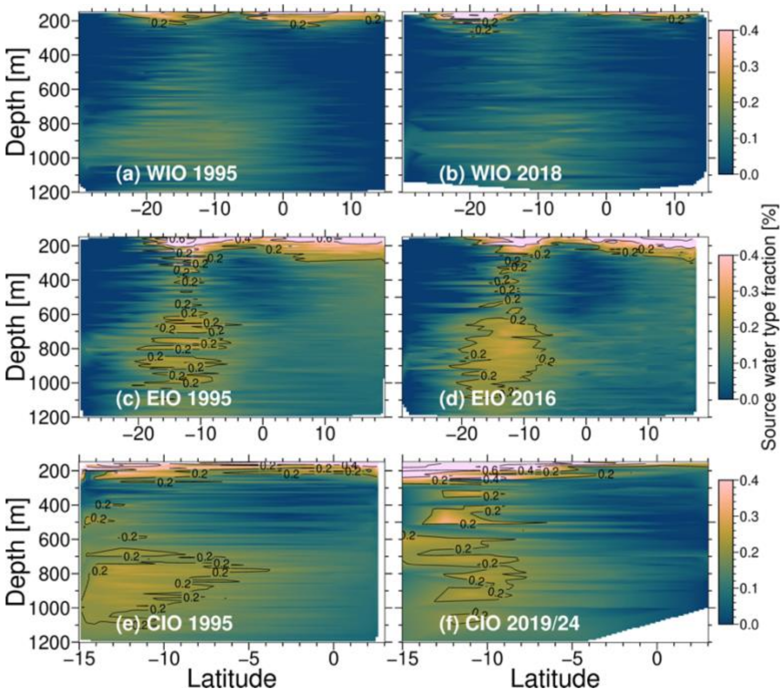

Figure 5: Temporal changes in Indonesian Throughflow Water (ITFW) fraction between 1995 and recent years across (a, b) western Indian Ocean (WIO) transect (c, d) eastern Indian Ocean (EIO) transect and (e, f) central Indian Ocean (CIO) transect.

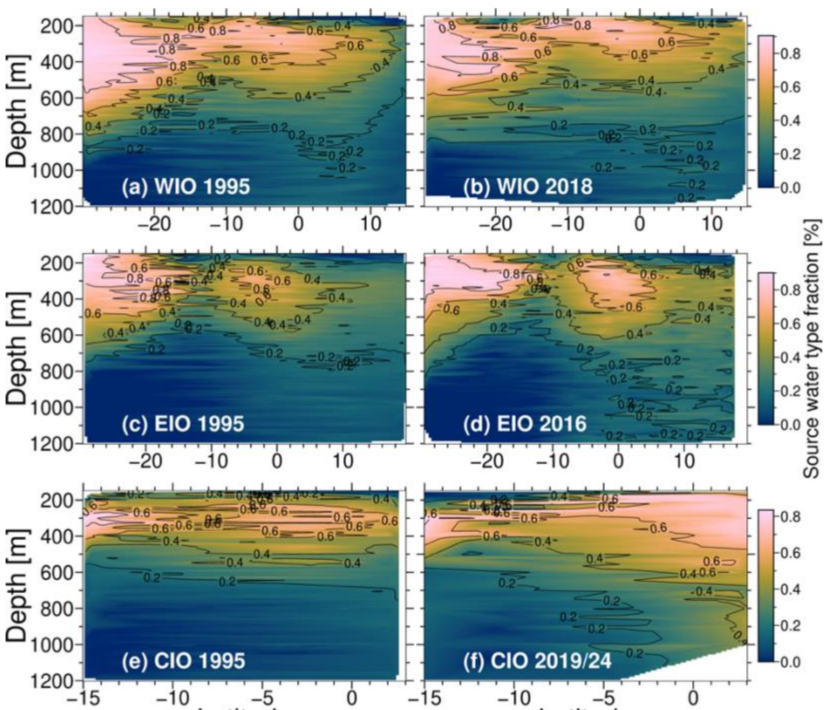

Figure 6: Temporal changes in Subtropical Surface Water (STSW) fraction between 1995 and recent years across (a, b) western Indian Ocean (WIO) transect, (c, d) eastern Indian Ocean (EIO) transect and (e, f) central Indian Ocean (CIO) transect.

3.2 Physical oxygen supply

Physical oxygen supply in the OMZs is mainly due to the supply and mixing of SWTs. Our results show that in western Indian Ocean and AS OMZ, physical oxygen supply rose from 193.2 to 196.5 µmol kg^{-1} and 135.80 to 143.80 µmol kg^{-1} respectively between 1995 and 2018 (Fig. 7c & 7a). While in the eastern Indian Ocean and BoB OMZ transects, oxygen supply rose from 191.3 to 198.4 µmol kg^{-1} and 175.7 to 184.3 µmol kg^{-1} respectively between 1995 and 2016 (Fig. 7c & 7b).

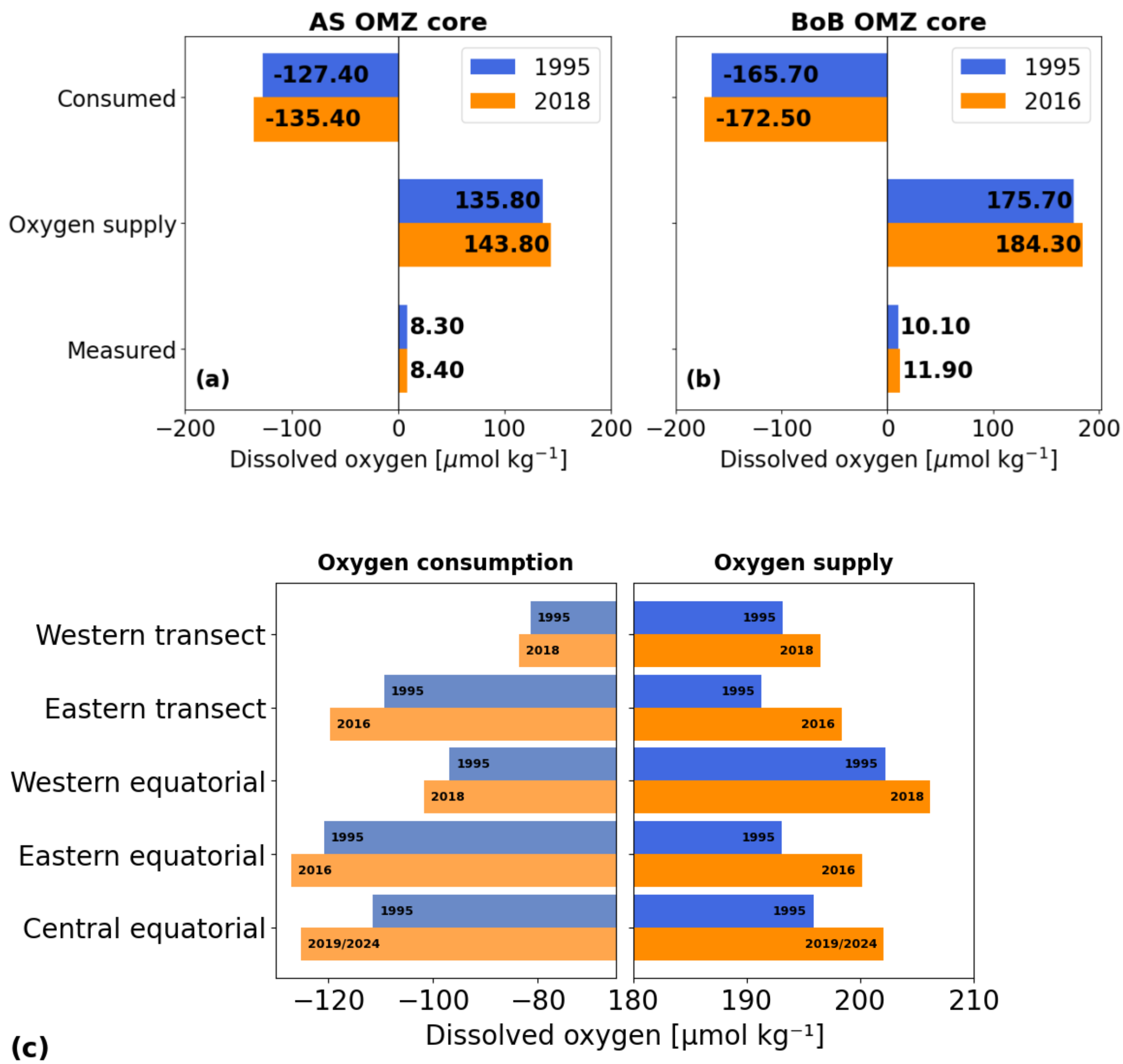

Figure 7: Mean oxygen supply (oxygen due to mixing), measured oxygen and biological oxygen consumption averaged over (a) Arabian Sea OMZ (O_2 < 20 µmol kg^{-1}, depth range 150–1000 m), (b) Bay of Bengal OMZ (O_2 < 20 µmol kg^{-1}, depth range 150–700 m), The measured oxygen values represent average dissolved oxygen within the OMZs at same depth range above (c) comparing oxygen supply and consumption across the western (1995 and 2018), eastern (1995 and 2016) and central equatorial transects (1995 and 2019/2024).

Analysis of equatorial transects also reveals an increase in physical oxygen supply around the equator, primarily due to increase in STSW and AAIW. Overall, the average physical oxygen supply increased from 202.2 to 206.2 µmol kg^{-1} in the western equatorial transect between 1995 and 2018, from 195.9 to 201.1 µmol kg^{-1} in the central equatorial region between 1995 and 2019/2024, and from 193.1 to 200.2 µmol kg^{-1} in the eastern equatorial transect between 1995 and 2016 (Fig. 7c). A cross section of the western and eastern transects reveals that both the core of the BoB OMZ and AS OMZ becomes shallower in 2016/2018 compared to 1995. The AS OMZ thickness shrank from 1092 m to 1025 m, while the BoB OMZ thickness shrank from 744 m to 733 m (Fig. 8). Overall, the increase in physical oxygen supply is more pronounced from approximately 15° S towards the northern Indian Ocean (Fig. 9). Our study reveals an increase in the physical oxygen supply in the Indian Ocean OMZs.

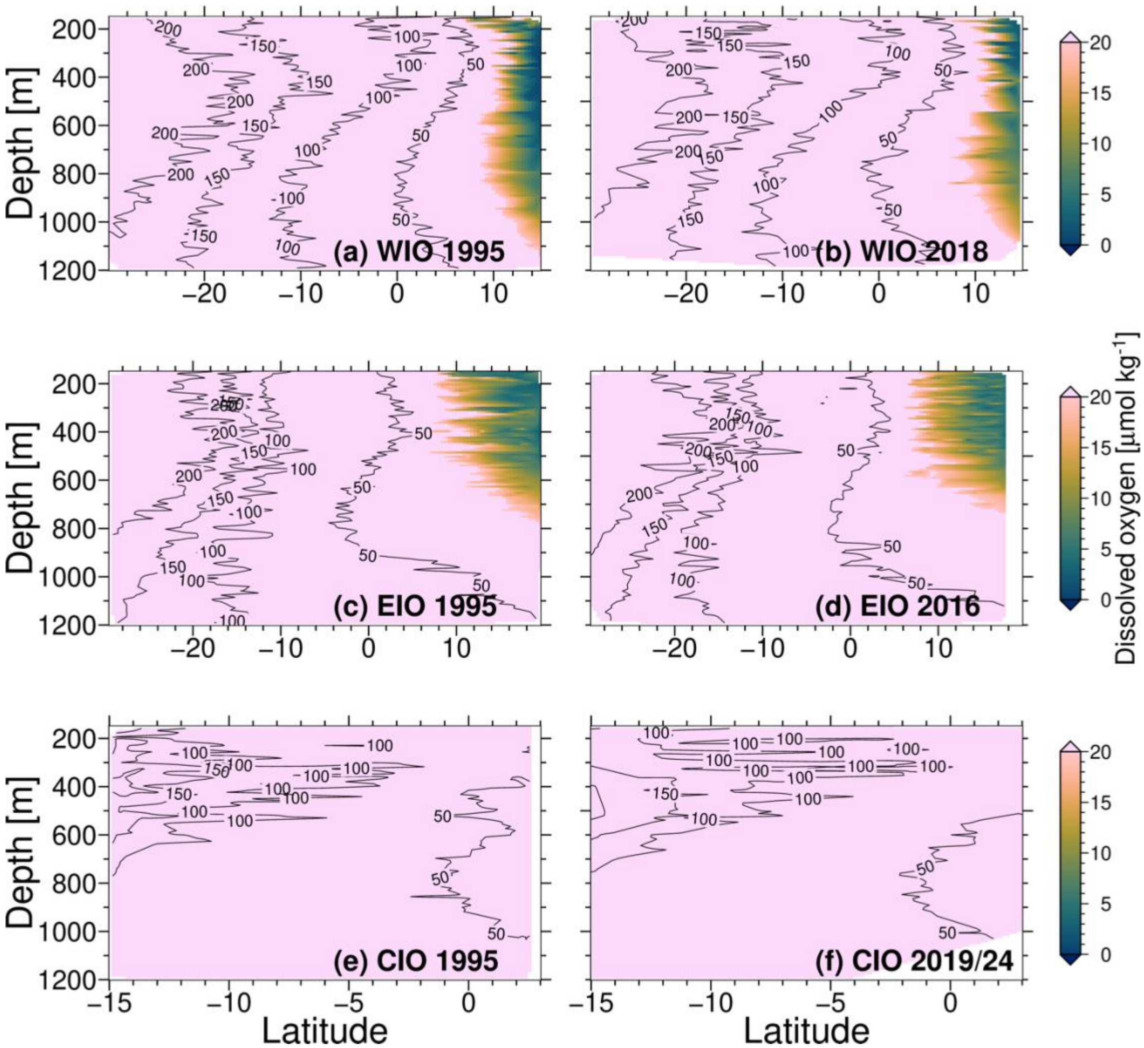

Figure 8: Temporal changes in measured oxygen concentration between 1995 and recent years based on analysis of GLODAPv2 data. (a, b) Western Indian Ocean (WIO) transect, (c, d) eastern Indian Ocean (EIO) transect and (e, f) central Indian Ocean (CIO) transect. With focus on the oxygen minimum zones.

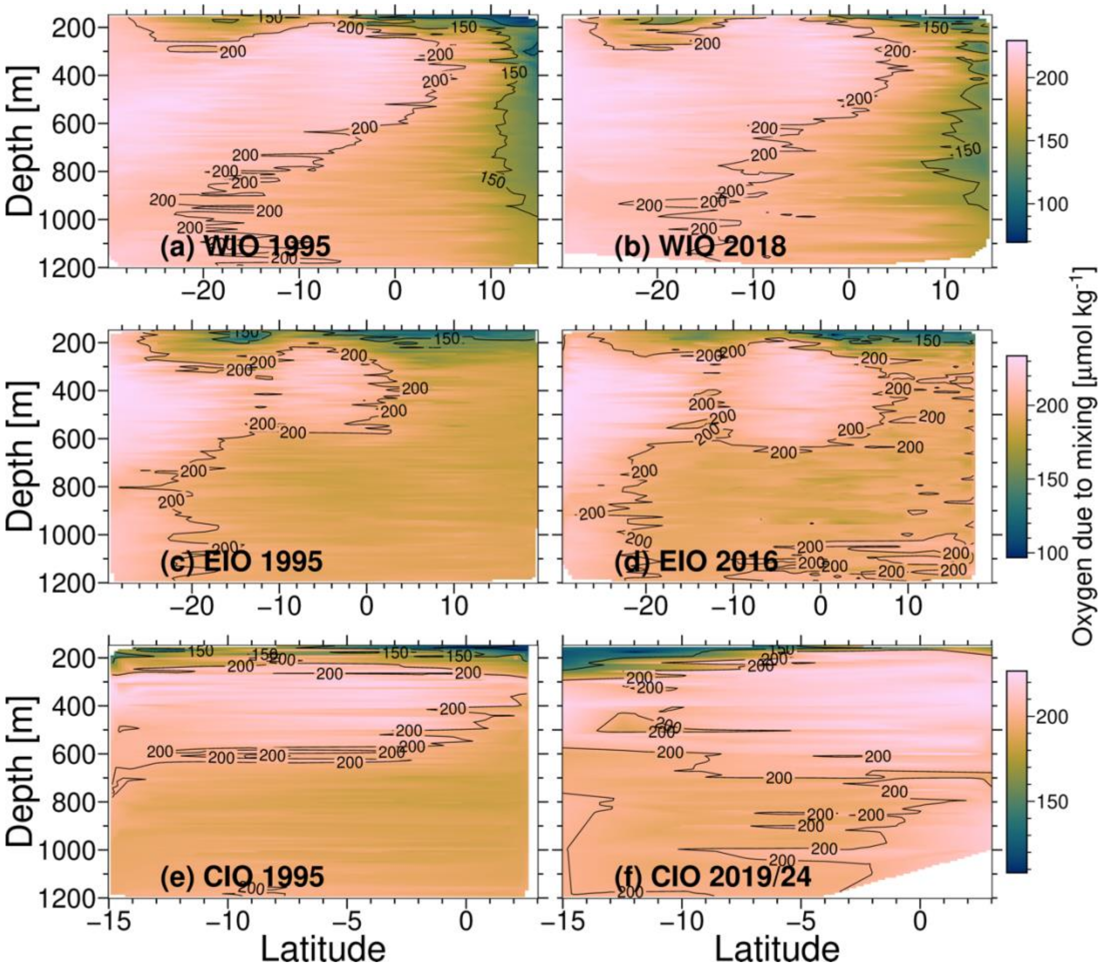

Figure 9: Temporal changes in physical oxygen supply (oxygen due to mixing) between 1995 and recent years across (a, b) western Indian Ocean (WIO) transect, (c, d) eastern Indian Ocean (EIO) transect and (e, f) central Indian Ocean (CIO) transect.

3.3 Biological oxygen consumption

In this section we quantify oxygen consumption to provide a clearer picture of the dissolved oxygen dynamics of the Indian Ocean OMZs. Analysis of data across the entire transects reveals an increase in biological oxygen consumption. In the western transect, oxygen consumption rose from -81.3 to -83.6 µmol kg^{-1} between 1995 and 2018, while in the eastern transect it rose from -110.2 to -119.6 µmol kg^{-1} between 1995 and 2016 (Fig. 7c). Similarly, the equatorial transects exhibited a comparable upward trend; biological oxygen consumption increased from -96.8 to -101.7 µmol kg^{-1} in the western equatorial transect between 1995 and 2018, from -111.4 to -125.1 µmol kg^{-1} in the central equatorial region between 1995 and 2019/2024, and from -120.8 to -127.1 µmol kg^{-1} in the eastern equatorial transect between 1995 and 2016 (Fig. 7c).

Furthermore, analysis indicates a significant increase in biological oxygen consumption in the core of both the AS OMZ and BoB OMZ. In the AS OMZ, oxygen consumption increased from an average of -127.4 µmol kg^{-1} in 1995 to -135.4 µmol kg^{-1} in 2018 (Fig. 7a), similarly, in the BoB OMZ, oxygen consumption rose from approximately -165.7 µmol kg^{-1} in 1995 to -172.5 µmol kg^{-1} in 2016 (Fig. 7b).

4 Discussion

The spatial distribution of SWTs in 1995 reveals clear regional differences in OMZ ventilation across the Indian Ocean. Since we considered only primary SWTs, these findings provide a slightly different perspective compared to previous studies. Earlier studies identified the ICW as the most prominent SWT in the AS OMZ, in association with the RSW and PGW (Schmidt et al., 2020; Rixen and Ittekkot, 2005; Acharya and Panigrahi, 2016; Hupe and Karstensen, 2000). However, the ICW originates through convective mixing in the southern Indian Ocean (Sverdrup et al., 1942) and it is also a mixture of STSW and ITFW (Schott and Mccreary Jr, 2001). The current SWTs composition in the Arabian Sea is therefore consistent with previous studies but enables for a direct assessment of the role of primary SWTs, rather than mixtures, in ventilating the OMZ. For example, in the AS OMZ in 1995 PGW contributes the most with 28%, while ITFW and STSW together contribute 30%, whereas, ITFW actually only contributes 6% while STSW 24%. Furthermore, our results suggest that in the mid-1990s, remote and equatorial SWTs such as mAABW, STSW and ITFW were prominent throughout the basin whereas the ITFW seems to influence the central and eastern transects more than the western transect, probably due to vicinity to the entry region of the ITFW into the Indian Ocean basin. The PGW played a more significant role in the western region and especially in the AS OMZ indicating that the AS OMZ receives substantial ventilation from marginal seas as already pointed out by Lachkar et al. (2019). The BoB OMZ on the other hand, relies more on remote SWTs such as STSW and mAABW.

4.1 Temporal changes in source water type contributions

The comparison of eOMP results based on the 1995 and the data from 2016–2024 indicate a net reduction in the influence of local and equatorial sources and an increased penetration of waters formed at higher southern latitudes into the OMZs which also includes a diminished influence from the ITF. The factors contributing to these changes will be discussed below.

4.1.1 Increased stratification and declining monsoon

All SWTs from the northern Indian Ocean which dominate the upper 300–450 m and the shallow MOC including PGW and RSW experienced a decline in the entire western, eastern and equatorial transects. The consistency of these results, despite the positive IOD phase in 2019, indicates that these changes in the composition of the water masses have occurred between the observation periods independently from the varying ENSO and IOD states. The decline in local SWTs in general may be attributed to increased stratification and reduced vertical mixing due to increased surface warming in the northern Indian Ocean (Sridevi et al., 2023; Helm et al., 2011; Roxy et al., 2020). Furthermore, the decline of PGW in the BoB OMZ can be attributed to decline in the summer monsoon (Roxy et al., 2015; Zhou et al., 2008) which can limit the lateral transport of water from the Arabian Sea to the Bay of Bengal through the southwest monsoon current (Fig.1).

4.1.2 Implications of the meridional overturning circulation

The increase in remote SWTs at the expense of the northern SWTs and the ITF at intermediate depth (150–1200 m) of the Indian Ocean and its OMZs indicates a reorganization of large-scale ocean circulation such as the global THC and the shallow Indian Ocean MOC. The decline of the global THC due to global warming has been reported (Caesar et al., 2021; de la Vara et al., 2022; Gou et al., 2024). This decline has led to the weakening of the ITF inflow in the Indian Ocean and the Agulhas leakage into the Atlantic Ocean (Großelindemann et al., 2024; Shen et al., 2023; Peng et al., 2023). Such a weakening of the cross-equatorial (zonal) flow, seem to have favored the northward (meridional) flow of remote SWTs along with the shallow Indian Ocean MOC into the northern Indian Ocean (Fig. 4, 5 and 6). This reorganization is evidenced by the increased percentage contribution of STSW, especially in the OMZ cores of both the Arabian Sea and the Bay of Bengal. Overall, there also seems to be a reduced influence of the deep cell of the Indian Ocean MOC at intermediate depths (150–1200 m), evident by the decline of mAABW in the western transect and in the OMZs' core. The overall observed adjustments in circulation patterns also means a southward shift from local to remote SWTs contributing to the OMZs.

These findings corresponds with studies by Ditkovsky et al. (2023) which also highlights that the southwest Indian Ocean experience increased influx of high-oxygenated waters supplied from the southern Indian Ocean gyre due to a decline in the contribution of the ITF. Despite inherent uncertainties in numerical modelling and our eOMP analysis, both approaches consistently capture this transition, lending confidence to the inferred shift in water mass contributions. As the individual SWTs have different oxygen concentrations, these variations also affect the physical supply of oxygen.

4.2 Physical oxygen supply

Our analysis reveals that the Indian Ocean OMZs have experienced an increase in physical oxygen supply due to an increased contribution from remote SWTs across all transects and a reduced influence from relatively oxygen-poor local and equatorial SWTs (e.g., PGW and ITFW). This aligns with model results suggesting oxygen increase in the AS OMZ is driven by a reorganization of the MOC (Ditkovsky et al., 2023; Lachkar et al., 2023; Oschlies et al., 2017; Vallivattathillam et al., 2023). Hence the climate-induced low ventilation of AS OMZ due to the reduced inflow of PGW (Lachkar et al., 2019) seems to have weakened. Furthermore, the Bay of Bengal also appears to benefit more from inflow of oxygen-rich remote SWTs, which in addition to salinity stratification, the occurrence of cyclonic, and anticyclonic eddies (Bhaskar et al., 2021) seems to be responsible for the oxygen stability in the BoB OMZ.

4.3 Biological oxygen consumption

The high oxygen consumption in the Indian Ocean OMZs has traditionally been attributed to monsoon-induced high primary productivity (Rixen et al., 1996; Wiggert et al., 2006). However, recent studies suggest a weakening of the summer monsoon (Zhou et al., 2008; Roxy et al., 2015). Additionally, model studies imply that increasing equatorial oxygen concentrations are caused by decreasing oxygen consumption (Kwiatkowski et al., 2020), which also aligns with declining primary productivity (PP) in the Arabian Sea/equatorial Indian Ocean since 2005 observed from analysis of PP data (Supplement Fig. S1). Despite this reported trend, our analysis shows an increasing oxygen consumption, suggesting that alternative mechanisms have been at play. One possible explanation for this increased biological oxygen consumption is a longer residence time of water masses in the Indian Ocean OMZs due to weaker upwelling slowing down the MOC. This means water masses are trapped within the Indian Ocean basin and its OMZs for longer period, prolonging its exposure to remineralization processes (Cavan et al., 2017; Rixen et al., 2020). Hence, it seems that the slowdown in the global THC (i.e., the associated reduced inflow of ITF as well as lower outflow via the Agulhas leakage) in addition to weakening of the monsoon have slowed down the MOC which finally seem to have increased the oxygen consumption by increasing the residence time of water in the OMZ. Due to the counteracting processes: enhanced physical oxygen supply and enhanced biological oxygen consumption the measured increase in dissolved oxygen in the GLODAPv2 data is relatively small, approximately 0.1 μmol kg^{-1} in the AS OMZ and on average 1.8 μmol kg^{-1} in the BoB OMZ (Fig. 7a & 7b). Hence, how the OMZs develop in future therefore depends, on both the reorganization of the SWTs and the velocity of the MOC.

4.4 Historical context of OMZ variability

Historical results obtained from the global atmosphere-ocean model and eddy-resolving regional models, indicates that the reduced inflow of oxygen-rich waters from the south has contributed to the intensification of the AS OMZ over the past 6,000 years as reported in a review by Rixen et al. (2020). Our results in line with model results (Vallivattathillam et al., 2023; Ditkovsky et al., 2023) suggest the opposite mechanism: an enhanced supply of oxygen-rich waters from the south caused the shrinking of the AS OMZ since 2013 (Liu et al., 2024). This trend reversal could be attributed to the reorganization of the MOC in response to global warming and the associated weakening of the ITF and the global THC as well as a decreasing monsoon-driven productivity. However, whether this trend will persists seem to depend on the competing influences of physical oxygen supply and biological oxygen consumption on the OMZ, driven by the reorganization and the slowdown of the MOC, respectively.

To place these recent changes in a broader temporal context, paleoceangraphic records indicate a strong link between climate changes in the north Atlantic Ocean and the AS OMZ on glacial and interglacial time scales (Altabet et al., 1999; Schulz et al., 1998; Suthhof et al., 2001). But in contrasts to our results a warming was associated with an intensification of the OMZ and cooling with a reduced intensification. However, on these paleo-time scales, climate changes are linked to changes in sea level (Rosenthal et al., 2003; Dinezio and Tierney, 2013). Decreasing sea levels must therefore have lowered the ITF during cooler phases, which in turn caused the enhanced transport of well-oxygenated waters from the south towards the north. Today, however, the reduced influx of the ITF is not caused by a drop in sea level, but by changes in circulation patterns. These changes are not yet well understood, but they imply that the current drivers of change differ from those in the past, although the mechanisms: an enhance meridional circulation at the expense of a weaker zonal circulation appear to be similar.

5 Summary and conclusion

Our study confirms a trend reversal in the expansion of the AS OMZ and also provides new evidence of the shrinkage of the BoB OMZ. It also advances our understanding of how distinct primary SWTs contribute to the ventilation of these OMZs in the past (i.e., 1995) compared to recent years. In line with other results, our findings reveal that the enhanced inflow of oxygen-rich remote SWTs increases physical oxygen supply. However, in contrast to other results our findings indicate an increased biological oxygen consumption, which partly offsets the effect of the increased oxygen supply on the oxygen concentrations in the OMZs. Nevertheless, the net result was still an overall increase in dissolved oxygen in both the AS OMZ and BoB OMZ. These shifts are likely linked to the reorganization and slowdown of the Indian Ocean MOC in response to global warming and the associated weakening of the ITF and the THC. In contrast to the present, where the ITF weakening is primarily caused by climate-driven circulation changes, past variation of the ITF was linked to extreme sea level changes on glacial interglacial time scale. However, the underlay mechanism remains the same: a reduced ITF favored the ventilation of the OMZs. Our findings will help improve the representation of the Indian Ocean OMZs in global models, while also indicating the need for continuous monitoring and high-resolution modelling studies to achieve a comprehensive understanding of long-term circulation and oxygen changes in these OMZs under global warming.

Data and code availability

The data and codes to reproduce our result are available for download here:
https://doi.org/10.5281/zenodo.19470323

Primary productivity data: https://catalogue.ceda.ac.uk/uuid/69b2c9c6c4714517ba10dab3515e4ee6/

Sea surface temperature data: https://psl.noaa.gov/data/gridded/data.noaa.oisst.v2.highres.html

Authors contributions

Cruise data collection: T.R, B.G, N.L Data curation: E.O. Data preparation, coding, and analysis: E.O. Funding acquisition: T.R, B.G. PYOMPA package development and code review: A.S. Writing: E.O. Reviews and editing: T.R, B.G, N.L., A.S.

Competing interests

The authors declare that they have no conflict of interest.

Acknowledgements

We appreciate the effort and contribution of the entire team who participated in the SONNE SO303 cruise in February 2024. Furthermore, many thanks to the German Federal Ministry of Education and Research (BMBF), this work was only possible because of their funding (grant number: 03G0303B). Finally, we appreciate the entire team at Leibniz Centre for Tropical Marine Research (ZMT), Bremen for providing a conducive environment and tools needed for research and learning.

References

Abbott, K. and Mahadevan, A.: Why Is the Monsoon Coastal Upwelling Signal Subdued in the Bay of Bengal?, Journal of Geophysical Research: Oceans, 129, e2024JC022023, https://doi.org/10.1029/2024JC022023, 2024.

Abram, N. J., Gagan, M. K., McCulloch, M. T., Chappell, J., and Hantoro, W. S.: Coral Reef Death During the 1997 Indian Ocean Dipole Linked to Indonesian Wildfires, Science, 301, 952-955, 2003.

Acharya, S. S. and Panigrahi, M. K.: Eastward shift and maintenance of Arabian Sea oxygen minimum zone: Understanding the paradox, Deep Sea Research Part I: Oceanographic Research Papers, 115, 240-252, 2016.

Altabet, M. A., Murray, D. W., and Prell, W. L.: Climatically linked oscillations in Arabian Sea denitrification over the past 1 my: Implications for the marine N cycle, Paleoceanography, 14, 732-743, 1999.

Anderson, L. A. and Sarmiento, J. L.: Redfield ratios of remineralization determined by nutrient data analysis, Global Biogeochem Cy, 8, 65-80, 1994.

Ayers, J. M., Strutton, P. G., Coles, V. J., Hood, R. R., and Matear, R. J.: Indonesian throughflow nutrient fluxes and their potential impact on Indian Ocean productivity, Geophysical Research Letters, 41, 5060-5067, 2014.

Bange, H. W., Naqvi, S. W. A., and Codispoti, L. A.: The nitrogen cycle in the Arabian Sea, Progress in Oceanography, 65, 145-158, 2005.

Banse, K., Naqvi, S., Narvekar, P., Postel, J., and Jayakumar, D.: Oxygen minimum zone of the open Arabian Sea: variability of oxygen and nitrite from daily to decadal timescales, Biogeosciences, 11, 2237-2261, 2014.

Beal, L. M., Ffield, A., and Gordon, A. L.: Spreading of Red Sea overflow waters in the Indian Ocean, Journal of Geophysical Research: Oceans, 105, 8549-8564, 2000.

Beal, L. M., Chereskin, T. K., Lenn, Y. D., and Elipot, S.: The sources and mixing characteristics of the Agulhas Current, Journal of physical oceanography, 36, 2060-2074, 2006.

Benson, B. B. and Krause Jr, D.: The concentration and isotopic fractionation of oxygen dissolved in freshwater and seawater in equilibrium with the atmosphere 1, Limnology and oceanography, 29, 620-632, 1984.

Benson, B. B. and Krause Jr., D.: The concentration and isotopic fractionation of gases dissolved in freshwater in equilibrium with the atmosphere. 1. Oxygen, Limnology and Oceanography, 25, 662-671, https://doi.org/10.4319/lo.1980.25.4.0662, 1980.

Bhaskar, T., Sarma, V. V. S. S., and Kumar, J. P.: Potential Mechanisms Responsible for Spatial Variability in Intensity and Thickness of Oxygen Minimum Zone in the Bay of Bengal, Journal of Geophysical Research Biogeosciences, 126, 10.1029/2021jg006341, 2021.

Bjerknes, J.: A possible response of the atmospheric Hadley circulation to equatorial anomalies of ocean temperature, Tellus, 18, 820-829, https://doi.org/10.1111/j.2153-3490.1966.tb00303.x, 1966.

Bjerknes, J.: Atmospheric Teleconnections from the Equatorial Pacific, Monthly Weather Review, 97, 163-172, 1969.

Bower, A. S., Hunt, H. D., and Price, J. F.: Character and dynamics of the Red Sea and Persian Gulf outflows, Journal of geophysical research: Oceans, 105, 6387-6414, 2000.

Breitburg, D. L., Grégoire, M., and Isensee, K.: The ocean is losing its breath: Declining oxygen in the world's ocean and coastal waters, 2018.

Bristow, L. A., Callbeck, C. M., Larsen, M., Altabet, M. A., Dekaezemacker, J., Forth, M., Gauns, M., Glud, R. N., Kuypers, M. M. M., Lavik, G., Milucka, J., Naqvi, S. W. A., Pratihary, A., Revsbech, N. P., Thamdrup, B., Treusch, A. H., and Canfield, D. E.: N2 production rates limited by nitrite availability in the Bay of Bengal oxygen minimum zone, Nature Geoscience, 10, 24 - 29, 10.1038/ngeo2847 http://www.nature.com/ngeo/journal/vaop/ncurrent/abs/ngeo2847.html#supplementary-information, 2017.

Brock, J. C., McClain, C. R., Luther, M. E., and Hay, W. W.: The Phytplankton Bloom in the Northwestern Arabian Sea During the Southwest Monsoon of 1979, Journal of Geophysical Research, 96, 20,623-620,642, 1991.

Brock, J. C., McClain, C. R., Anderson, D. M., Prell, W. L., and Hay, W. W.: Southwest Monsoon Circulation and Environments of Recent Planktonic Foraminifera in the Northwestern Arabian Sea, Paleoceanography, 7, 799-813, 1992.

Broecker, W. S.: The Great Ocean Conveyor, Oceanography, 4, 79-89, 1991.

Cavan, E. L., Trimmer, M., Shelley, F., and Sanders, R.: Remineralization of particulate organic carbon in an ocean oxygen minimum zone, Nature Communications, 8, 14847, 2017.

Chavez, F. P. and Messié, M.: A comparison of Eastern Boundary Upwelling Ecosystems, Progress in Oceanography, 83, 80-96, 2009.

Chinni, V., Singh, S. K., Bhushan, R., Rengarajan, R., and Sarma, V.: Spatial variability in dissolved iron concentrations in the marginal and open waters of the Indian Ocean, Marine Chemistry, 208, 11-28, 2019.

Coatanoan, C., Metzl, N., Fieux, M., and Coste, B.: Seasonal water mass distribution in the Indonesian throughflow entering the Indian Ocean, Journal of Geophysical Research: Oceans, 104, 20801-20826, 1999.

de Brauwere, A., Jacquet, S. H., De Ridder, F., Dehairs, F., Pintelon, R., Schoukens, J., and Baeyens, W.: Water mass distributions in the Southern Ocean derived from a parametric analysis of mixing water masses, Journal of Geophysical Research: Oceans, 112, 2007.

DiNezio, P. N. and Tierney, J. E.: The effect of sea level on glacial Indo-Pacific climate, Nature Geoscience, 6, 485-491, 2013.

Ditkovsky, S., Resplandy, L., and Busecke, J.: Unique ocean circulation pathways reshape the Indian Ocean oxygen minimum zone with warming, Biogeosciences, 20, 4711-4736, 2023.

Durgadoo, J. V., Rühs, S., Biastoch, A., and Böning, C. W. B.: Indian Ocean sources of Agulhas leakage, Journal of Geophysical Research: Oceans, n/a-n/a, 10.1002/2016JC012676, 2017.

Duteil, O. and Oschlies, A.: Sensitivity of Simulated Extent and Future Evolution of Marine Suboxia to Mixing Intensity, Geophysical Research Letters, 38, n/a-n/a, 10.1029/2011gl046877, 2011.

Ekau, W., Auel, H., Pörtner, H. O., and Gilbert, D.: Impacts of hypoxia on the structure and processes in pelagic communities (zooplankton, macro-invertebrates and fish), Biogeosciences, 7, 1669-1699, 10.5194/bg-7-1669-2010, 2010.

Fine, R. A.: Circulation of Antarctic intermediate water in the South Indian Ocean, Deep Sea Research Part I: Oceanographic Research Papers, 40, 2021-2042, 1993.

Gadgil, S., Rajeevan, M., and Francis, P. A.: Monsoon variability: Links to major oscillations over the equatorial Pacific and Indian oceans, Current science, 93, 182-194, 2007.

Gaye, B., Andersch, T., Bartsch, P., Cosmus, H., Dähnke, K., Dasbach, D., Eisnecker, P., Gök, I., Harms, N., Hubert-Huard, R., Hüge, F., John, F., Keuter, S., Kretzschmann, L., Lahajnar, N., Lisitano, L., Lüdmann, T., Markfort, G., Meiritz, L., Oldhaver, M., Penopp, J., Prien, R. D., Rixen, T., Ruda, L., Sanders, T., Schulz, G., Schulz, H., Siccha, M., Sommer, M., Sorge, Y., and Waniek, J. J.: BIOGeochemistry in the equatorial INdian Ocean - BIOGIN-IIOE2, Cruise No. SO303, 23.01.2024 - 19.02.2024, La Réunion (France) - Colombo (Sri Lanka), Begutachtungspanel Forschungsschiffe;, Bonn2510-764X, 1-81, 10.48433/cr_so303, 2024.

Godfrey, J. S.: The effect of the Indonesian throughflow on ocean circulation and heat exchange with the atmosphere: A review, Journal of Geophysical Research, 101, 12,217-212,237, 1996.

Goes, J., Tian, H., Gomes, H. d. R., Anderson, O., Al-Hashmi, K., deRada, S., Luo, H., Al-Kharusi, L., Al-Azri, A., and Martinson, D.: Ecosystem state change in the Arabian Sea fuelled by the recent loss of snow over the Himalayan-Tibetan Plateau region, Sci. Rep., 10, 7422, 2020.

Gordon, A. L.: Interocean Exchange of Thermocline Water, J. Geophys. Res., 91, 5037-5046, 10.1029/JC091iC04p05037, 1986.

Gordon, A. L., Susanto, R. D., and Vranes, K.: Cool Indonesian throughflow as a consequence of restricted surface layer flow, Nature, 425, 824-828, 2003.

Gordon, A. L., Sprintall, J., Van Aken, H. M., Susanto, D., Wijffels, S., Molcard, R., Ffield, A., Pranowo, W., and Wirasantosa, S.: The Indonesian throughflow during 2004–2006 as observed by the INSTANT program, Dynamics of Atmospheres and Oceans, 50, 115-128, http://dx.doi.org/10.1016/j.dynatmoce.2009.12.002, 2010.

Großelindemann, H., Castruccio, F. S., Danabasoglu, G., and Biastoch, A.: Long-term Variability and Trends of Agulhas Leakage and its Impacts on the Global Overturning, EGUsphere, 2024.

Haake, B., Ittekkot, V., Rixen, T., Ramaswamy, V., Nair, R. R., and Curry, W. B.: Seasonality and interannual variability of particle fluxes to the deep Arabian Sea, Deep Sea Research I, 40, 1323-1344, 1993.

Haine, T. W., Watson, A. J., Liddicoat, M. I., and Dickson, R. R.: The flow of Antarctic bottom water to the southwest Indian Ocean estimated using CFCs, Journal of Geophysical Research: Oceans, 103, 27637-27653, 1998.

Harms, N. C., Lahajnar, N., Gaye, B., Rixen, T., Dähnke, K., Ankele, M., Schwarz-Schampera, U., and Emeis, K.-C.: Nutrient distribution and nitrogen and oxygen isotopic composition of nitrate in water masses of the subtropical southern Indian Ocean, Biogeosciences, 16, 2715-2732, 2019.

Helm, K. P., Bindoff, N. L., and Church, J. A.: Observed decreases in oxygen content of the global ocean, Geophysical Research Letters, 38, 2011.

Hupe, A. and Karstensen, J.: Redfield stoichiometry in Arabian Sea subsurface waters, Global Biogeochem Cy, 14, 357-372, 2000.

Water mass ages based on GLODAPv2 data product (NCEI Accession 0226793): https://doi.org/10.25921/xp33-q351., last

Johnson, G. C.: Quantifying Antarctic bottom water and North Atlantic deep water volumes, Journal of Geophysical Research: Oceans, 113, 2008.

Johnson, K. S., Riser, S. C., and Ravichandran, M.: Oxygen variability controls denitrification in the Bay of Bengal oxygen minimum zone, Geophysical Research Letters, 46, 804-811, 2019.

Kulk, G., Platt, T., Dingle, J., Jackson, T., Jönsson, B. F., Bouman, H. A., Babin, M., Brewin, R. J., Doblin, M., and Estrada, M.: Primary production, an index of climate change in the ocean: satellite-based estimates over two decades, Remote Sensing, 12, 826, 2020.

Kumar, S. P. and Prasad, T.: Formation and spreading of Arabian Sea high-salinity water mass, Journal of Geophysical Research: Oceans, 104, 1455-1464, 1999.

Kwiatkowski, L., Torres, O., Bopp, L., Aumont, O., Chamberlain, M., Christian, J. R., Dunne, J. P., Gehlen, M., Ilyina, T., John, J. G., Lenton, A., Li, H., Lovenduski, N. S., Orr, J. C., Palmieri, J., Santana-Falcón, Y., Schwinger, J., Séférian, R., Stock, C. A., Tagliabue, A., Takano, Y., Tjiputra, J., Toyama, K., Tsujino, H., Watanabe, M., Yamamoto, A., Yool, A., and Ziehn, T.: Twenty-first century ocean warming, acidification, deoxygenation, and upper-ocean nutrient and primary production decline from CMIP6 model projections, Biogeosciences, 17, 3439-3470, 10.5194/bg-17-3439-2020, 2020.

Lachkar, Z., Lévy, M., and Smith, K. S.: Strong intensification of the Arabian Sea oxygen minimum zone in response to Arabian Gulf warming, Geophysical Research Letters, 46, 5420-5429, 2019.

Lachkar, Z., Lévy, M., and Smith, S.: Intensification and deepening of the Arabian Sea oxygen minimum zone in response to increase in Indian monsoon wind intensity, Biogeosciences, 15, 159-186, 10.5194/bg-15-159-2018, 2018.

Lachkar, Z., Levy, M., Hailegeorgis, D., and Vallivattathillam, P.: Differences in recent and future trends in the Arabian Sea oxygen minimum zone: processes and uncertainties, Front Mar Sci, 10, 1122043, 2023.

Lauvset, S. K., Lange, N., Tanhua, T., Bittig, H. C., Olsen, A., Kozyr, A., Alin, S., Álvarez, M., Azetsu-Scott, K., Barbero, L., Becker, S., Brown, P. J., Carter, B. R., da Cunha, L. C., Feely, R. A., Hoppema, M., Humphreys, M. P., Ishii, M., Jeansson, E., Jiang, L. Q., Jones, S. D., Lo Monaco, C., Murata, A., Müller, J. D., Pérez, F. F., Pfeil, B., Schirnick, C., Steinfeldt, R., Suzuki, T., Tilbrook, B., Ulfsbo, A., Velo, A., Woosley, R. J., and Key, R. M.: GLODAPv2.2022: the latest version of the global interior ocean biogeochemical data product, Earth Syst. Sci. Data, 14, 5543-5572, 10.5194/essd-14-5543-2022, 2022.

Lee, T., Fukumori, I., Menemenlis, D., Xing, Z., and Fu, L.-L.: Effects of the Indonesian throughflow on the Pacific and Indian Oceans, Journal of Physical Oceanography, 32, 1404-1429, 2002.

Liu, T., Qiu, Y., Lin, X., Ni, X., Wang, L., Li, H., and Jing, C.: Dissolved oxygen recovery in the oxygen minimum zone of the Arabian Sea in recent decade as observed by BGC-argo floats, Geophysical Research Letters, 51, e2024GL108841, 2024.

Malone, T., Azzaro, M., Bode, A., Brown, E., Duce, R., Kamykowski, D., Kang, S., Kedong, Y., Thorndyke, M., and Wang, J.: Primary Production, Cycling of Nutrients, Surface Layer and Plankton, Centro Oceanográfico de A Coruña, 2015.

Mantyla, A. W. and Reid, J. L.: On the origins of deep and bottom waters of the Indian Ocean, Journal of Geophysical Research: Oceans, 100, 2417-2439, 1995.

Menezes, V. V., Macdonald, A. M., and Schatzman, C.: Accelerated freshening of Antarctic Bottom Water over the last decade in the Southern Indian Ocean, Science Advances, 3, e1601426, 10.1126/sciadv.1601426, 2017.

Narvekar, J., Kesserkar, P., Sreejith, K., Fernandes, L., and Kumar, S. P.: Recent oxygenation of oxygen minimum zone in the Arabian Sea and possible causes, Prog Oceanogr, 103600, 2025.

Nayak, A. A., Vinayachandran, P., and George, J. V.: Arabian Sea high salinity core supplies oxygen to Bay of Bengal oxygen minimum zone, arXiv preprint arXiv:2406.10571, 2024.

Olsen, A., Lange, N., Key, R. M., Tanhua, T., Álvarez, M., Becker, S., Bittig, H. C., Carter, B. R., Cotrim da Cunha, L., Feely, R. A., van Heuven, S., Hoppema, M., Ishii, M., Jeansson, E., Jones, S. D., Jutterström, S., Karlsen, M. K., Kozyr, A., Lauvset, S. K., Lo Monaco, C., Murata, A., Pérez, F. F., Pfeil, B., Schirnick, C., Steinfeldt, R., Suzuki, T., Telszewski, M., Tilbrook, B., Velo, A., and Wanninkhof, R.: GLODAPv2.2019 – an update of GLODAPv2, Earth Syst. Sci. Data, 11, 1437-1461, 10.5194/essd-11-1437-2019, 2019.

Oschlies, A., Brandt, P., Stramma, L., and Schmidtko, S.: Drivers and mechanisms of ocean deoxygenation, Nature Geoscience, 11, 467-473, 10.1038/s41561-018-0152-2, 2018.

Oschlies, A., Duteil, O., Getzlaff, J., Koeve, W., Landolfi, A., and Schmidtko, S.: Patterns of deoxygenation: sensitivity to natural and anthropogenic drivers, Philosophical Transactions of the Royal Society A: Mathematical, Physical and Engineering Sciences, 375, 20160325, 2017.

Parvathi, V., Thadathil, P., Rajkumar, M., Prasannakumar, S., Muraleedharan, P., Ravichandran, M., Rao, R., and Gopalakrishna, V.: Quality of temperature and salinity data from Argo profiling floats in the Bay of Bengal, 2014.

Peng, Q., Xie, S.-P., Huang, R. X., Wang, W., Zu, T., and Wang, D.: Indonesian throughflow slowdown under global warming: Remote AMOC effect versus regional surface forcing, Journal of Climate, 36, 1301-1318, 2023.

Phillips, H. E., Tandon, A., Furue, R., Hood, R., Ummenhofer, C. C., Benthuysen, J. A., Menezes, V., Hu, S., Webber, B., Sanchez-Franks, A., Cherian, D., Shroyer, E., Feng, M., Wijesekera, H., Chatterjee, A., Yu, L., Hermes, J., Murtugudde, R., Tozuka, T., Su, D., Singh, A., Centurioni, L., Prakash, S., and Wiggert, J.: Progress in understanding of Indian Ocean circulation, variability, air–sea exchange, and impacts on biogeochemistry, Ocean Sci., 17, 1677-1751, 10.5194/os-17-1677-2021, 2021.

Poole, R. and Tomczak, M.: Optimum multiparameter analysis of the water mass structure in the Atlantic Ocean thermocline, Deep Sea Research Part I: Oceanographic Research Papers, 46, 1895-1921, 1999.

Prasad, T., Ikeda, M., and Kumar, S. P.: Seasonal spreading of the Persian Gulf Water mass in the Arabian Sea, Journal of Geophysical Research: Oceans, 106, 17059-17071, 2001.

Reichart, G. J., Nortier, J., Versteegh, G., and Zachariasse, W. J.: Periodical breakdown of the Arabian Sea oxygen minimum zone caused by deep convective mixing, 2002.

Rixen, T. and Ittekkot, V.: Nitrogen deficits in the Arabian Sea, implications from a three component mixing analysis, Deep Sea Research Part II: Topical Studies in Oceanography, 52, 1879-1891, 2005.

Rixen, T., Gaye, B., and Emeis, K.-C.: The monsoon, carbon fluxes, and the organic carbon pump in the northern Indian Ocean, Prog Oceanogr, 175, 24-39, https://doi.org/10.1016/j.pocean.2019.03.001, 2019.

Rixen, T., Baum, A., Gaye, B., and Nagel, B.: Seasonal and interannual variations in the nitrogen cycle in the Arabian Sea, Biogeosciences, 11, 5733-5747, 2014.

Rixen, T., Haake, B., Ittekkot, V., Guptha, M., Nair, R., and Schlüssel, P.: Coupling between SW monsoon-related surface and deep ocean processes as discerned from continuous particle flux measurements and correlated satellite data, Journal of Geophysical Research: Oceans, 101, 28569-28582, 1996.

Rixen, T., Ittekkot, V., Herundi, B., Wetzel, P., Maier-Reimer, E., and Gaye-Haake, B.: ENSO-driven carbon see saw in the Indo-Pacific, Journal of Geophysical Research Letters, 33, L07606, 10.1029/2005GL024965, 2006.

Rixen, T., Cowie, G., Gaye, B., Goes, J., do Rosário Gomes, H., Hood, R. R., Lachkar, Z., Schmidt, H., Segschneider, J., and Singh, A.: Reviews and syntheses: Present, past, and future of the oxygen minimum zone in the northern Indian Ocean, Biogeosciences, 17, 6051-6080, 10.5194/bg-17-6051-2020, 2020.

Rosenthal, Y., Oppo, D. W., and Linsley, B. K.: The amplitude and phasing of climate change during the last deglaciation in the Sulu Sea, western equatorial Pacific, Geophysical Research Letters, 30, 2003.

Roxy, M., Gnanaseelan, C., Parekh, A., Chowdary, J. S., Singh, S., Modi, A., Kakatkar, R., Mohapatra, S., Dhara, C., and Shenoi, S.: Indian ocean warming, Assessment of climate change over the Indian region: a report of the Ministry of Earth Sciences (MoES), Government of India, 191-206, 2020.

Roxy, M. K., Ritika, K., Terray, P., Murtugudde, R., Ashok, K., and Goswami, B.: Drying of Indian subcontinent by rapid Indian Ocean warming and a weakening land-sea thermal gradient, Nature communications, 6, 7423, 2015.

Rudnickas, D., Palter, J. B., Hebert, D., and Rossby, T.: Isopycnal Mixing in the North Atlantic Oxygen Minimum Zone Revealed by RAFOS Floats, Journal of Geophysical Research Oceans, 124, 6478-6497, 10.1029/2019jc015148, 2019.

Sabu, P., George, J. V., Anilkumar, N., Chacko, R., Valsala, V., and Achuthankutty, C.: Observations of watermass modification by mesoscale eddies in the subtropical frontal region of the Indian Ocean sector of Southern Ocean, Deep Sea Research Part II: Topical Studies in Oceanography, 118, 152-161, 2015.

Saenko, O. A. and Weaver, A. J.: Importance of wind-driven sea ice motion for the formation of Antarctic Intermediate Water in a global climate model, Geophysical Research Letters, 28, 4147-4150, 2001.

Saji, N. H., Goswami, B. N., Vinayachandran, P. N., and Yamagata, T.: A dipole mode in the tropical Inian Ocean, Nature, 401, 360-363, 1999.

Sarmiento, J. L., Gruber, N., Brzezinski, M. A., and Dunne, J. P.: High-latitude controls of thermocline nutrients and low latitude biological productivity, Nature, 427, 56-60, 2004.

Sastry, J. S. and D'Souza, R. S.: Upwelling & Upward Mixing in the Arabian Sea, Indian Journal of Marine Sciences, 1, 17-27, 1972.

Schmidt, H., Czeschel, R., and Visbeck, M.: Seasonal Variability of the Arabian Sea Intermediate Circulation and Its Impact on Seasonal Changes of the Upper Oxygen Minimum Zone, Ocean Science, 16, 1459-1474, 10.5194/os-16-1459-2020, 2020.

Schmidt, H., Getzlaff, J., Löptien, U., and Oschlies, A.: Causes of uncertainties in the representation of the Arabian Sea oxygen minimum zone in CMIP5 models, Ocean Sci., 17, 1303-1320, 10.5194/os-17-1303-2021, 2021.

Schmidtko, S., Stramma, L., and Visbeck, M.: Decline in global oceanic oxygen content during the past five decades, Nature, 542, 335-339, 2017.

Schott, F. A. and McCreary Jr, J. P.: The monsoon circulation of the Indian Ocean, Prog Oceanogr, 51, 1-123, 2001.

Schott, F. A., Xie, S.-P., and McCreary Jr, J. P.: Indian Ocean circulation and climate variability, Reviews of Geophysics, 47, https://doi.org/10.1029/2007RG000245, 2009.

Schulz, G., Dähnke, K., Sanders, T., Penopp, J., Bange, H. W., Czeschel, R., and Gaye, B.: Nitrogen dynamics and nitrate stable isotopes indicate nitrogen loss in the Bay of Bengal, EGUsphere, 2025, 1-27, 10.5194/egusphere-2025-1660, 2025.

Schulz, H., Von Rad, U., Erlenkeuser, H., and von Rad, U.: Correlation between Arabian Sea and Greenland climate oscillations of the past 110,000 years, Nature, 393, 54-57, 1998.

Sengupta, S., Parekh, A., Chakraborty, S., Ravi Kumar, K., and Bose, T.: Vertical variation of oxygen isotope in Bay of Bengal and its relationships with water masses, Journal of Geophysical Research: Oceans, 118, 6411-6424, 2013.

Sharma, G. S.: Upwelling Off the Soutwest Coast of India, Indian Journal of Marine Sciences, 7, 209-218, 1978.

Shen, C., Moore, J. C., Kuswanto, H., and Zhao, L.: The Indonesian Throughflow circulation under solar geoengineering, Earth System Dynamics, 14, 1317-1332, 2023.

Shetye, S. R., Gouveia, A. D., Shenoi, S. S. C., Sundar, D., Michael, G. S., Almeida, A. M., and Santanam, K.: Hydrography and circulation off the west coast of India during the Southwest Monsoon 1987, Journal of Marine Research, 48, 359-378, 1990.

Shrikumar, A., Lawrence, R., and Casciotti, K. L.: PYOMPA technical note, ESS Open Archive eprints, 105, essoar. 10507053, 2022.

Sigman, D. M. and Hain, M. P.: The biological productivity of the ocean, Nature Education Knowledge, 3, 21, 2012.

Singh, S. P., Singh, S. K., Goswami, V., Bhushan, R., and Rai, V. K.: Spatial distribution of dissolved neodymium and εNd in the Bay of Bengal: Role of particulate matter and mixing of water masses, Geochimica et Cosmochimica Acta, 94, 38-56, 2012.

Sokolov, S. and Rintoul, S. R.: Structure of Southern Ocean fronts at 140 E, Journal of Marine Systems, 37, 151-184, 2002.

Song, Q., Gordon, A. L., and Visbeck, M.: Spreading of the Indonesian throughflow in the Indian Ocean, Journal of Physical Oceanography, 34, 772-792, 2004.

Sridevi, B. and Sarma, V.: A revisit to the regulation of oxygen minimum zone in the Bay of Bengal, Journal of Earth System Science, 129, 1-7, 2020.

Sridevi, B., Sabira, S., and Sarma, V.: Impact of ocean warming on net primary production in the northern Indian Ocean: role of aerosols and freshening of surface ocean, Environmental Science and Pollution Research, 30, 53616-53634, 2023.

Stramma, L., Johnson, G. C., Sprintall, J., and Mohrholz, V.: Expanding oxygen-minimum zones in the tropical oceans, Science, 320, 655-658, 10.1126/science.1153847, 2008.

Stramma, L., Schmidtko, S., Levin, L. A., and Johnson, G. C.: Ocean oxygen minima expansions and their biological impacts, Deep Sea Research Part I: Oceanographic Research Papers, 57, 587-595, https://doi.org/10.1016/j.dsr.2010.01.005, 2010.

Stramma, L., Brandt, P., Schott, F., Quadfasel, D., and Fischer, J.: Winter and summer monsoon water mass, heat and freshwater transport changes in the Arabian Sea near 8° N, Deep Sea Research Part II: Topical Studies in Oceanography, 49, 1173-1195, 2002.

Susanto, R. D., Gordon, A. L., and Zengh, Q.: Upwelling along the coasts of Java and Sumatra and its relation to ENSO, Journal of Geophysical Research Letters, 28, 1599-1602, 2001a.

Susanto, R. D., Gordon, A. L., and Zengh, Q.: Upwelling along the coasts of Java and Sumatra and its relation to ENSO, Journal of Marine Research Letters, 28, 1599-1602, 2001b.

Suthhof, A., Ittekkot, V., and Gaye-Haake, B.: Millenial-scale oscillation of denitrification intensitiy in the Arabian Sea during the late Quaternary and its potential influence on atmospheric N_2O and global climate, Global Biogeochem Cy, 15, 637-650, 2001.

Sverdrup, H. U.: On the Explanation of the Oxygen Minima and Maxima in the Oceans1), ICES Journal of Marine Science, 13, 163-172, 10.1093/icesjms/13.2.163, 1938.

Sverdrup, H. U., Johnson, M. W., and Fleming, R. H.: The Oceans: Their physics, chemistry, and general biology, 8, Prentice-Hall New York1942.

Talley, L. D.: Antarctic Intermediate Water in the South Atlantic, in: The South Atlantic: Present and Past Circulation, Springer Berlin Heidelberg, Berlin, Heidelberg, 219-238, 10.1007/978-3-642-80353-6_11, 1996.

Talley, L. D.: Closure of the global overturning circulation through the Indian, Pacific, and Southern Oceans: Schematics and transports, Oceanography, 26, 80-97, 2013.

Tchernia, P.: Descriptive Regional Oceanography, Pergamon Press1980.

Tomczak, M.: Some historical, theoretical and applied aspects of quantitative water mass analysis, 1999.

Tomczak, M. and Large, D. G.: Optimum multiparameter analysis of mixing in the thermocline of the eastern Indian Ocean, Journal of Geophysical Research: Oceans, 94, 16141-16149, 1989.

Vallivattathillam, P., Lachkar, Z., and Lévy, M.: Shrinking of the Arabian Sea oxygen minimum zone with climate change projected with a downscaled model, Frontiers in Marine Science, 10, ARTN 1123739
10.3389/fmars.2023.1123739, 2023.

Vaquer-Sunyer, R. and Duarte, C. M.: Thresholds of hypoxia for marine biodiversity, Proceedings of the National Academy of Sciences, 105, 15452, 10.1073/pnas.0803833105, 2008.

Vianello, P., Ansorge, I., Rouault, M., and Ostrowski, M.: Transport and transformation of surface water masses across the Mascarene Plateau during the Northeast Monsoon season, African Journal of Marine Science, 39, 453-466, 2017.

Webster, P. J., Moore, A. M., Loschnigg, J. P., and Leben, R. R.: Coupled ocean-atmosphere dynamics in the Indian Ocean during 1997-98, Nature, 401, 356-360, 1999.

Wiggert, J., Murtugudde, R., and Christian, J.: Annual ecosystem variability in the tropical Indian Ocean: Results of a coupled bio-physical ocean general circulation model, Deep Sea Research Part II: Topical Studies in Oceanography, 53, 644-676, 2006.

Wyrtki, K.: Physical Oceanography of the Indian Ocean, in: The Biology of the Indian Ocean, edited by: Zeitschel, B., Springer Verlag, Berlin, Heidelberg, New York, 18-36, 1973.

Wyrtki, K., Bennett, E. B., and Rochford, D. J.: Oceanographic atlas of the international Indian Ocean expedition, (No Title), 1971.

You, Y.: Intermediate water circulation and ventilation of the Indian Ocean derived from water-mass contributions, 1998.

Yu, Z., Colin, C., Ma, R., Meynadier, L., Wan, S., Wu, Q., Kallel, N., Sepulcre, S., Dapoigny, A., and Bassinot, F.: Antarctic Intermediate Water penetration into the Northern Indian Ocean during the last deglaciation, Earth and Planetary Science Letters, 500, 67-75, 2018.

Zhou, T., Yu, R., Li, H., and Wang, B.: Ocean forcing to changes in global monsoon precipitation over the recent half-century, Journal of Climate, 21, 3833-3852, 2008.